Tripodal transmembrane transporters for bicarbonate

Nathalie Busschaert, Philip A. Gale,* Cally J.E. Haynes, Mark E. Light, Stephen J. Moore, Christine C. Tong, Jeffery T. Davis and William A. Harrell

Electronic Supplementary Information

Supplentary Information

General Remarks

^{1}H NMR (300 MHz) and ^{13}C{^{1}H} NMR (75 MHz) were determined on a Bruker AV300 spectrometer. Chemical shifts for ^{1}H NMR are reported in parts per million (ppm), calibrated to the solvent peak set. The following abbreviations are used for spin multiplicity: s = singlet, d = doublet, t = triplet, m = multiplet. Chemical shifts for ^{13}C{^{1}H} NMR are reported in ppm, relative to the central line of a septet at δ = 39.52 ppm for DMSO-d_6. Infrared (IR) spectra were recorded on a Matterson Satellite (ATR). FTIR are reported in wavenumbers (cm^{-1}). HRMS(ES) spectra were recorded using a Bruker Apex III spectrometer and reported as *m/z* (relative intensity). All solvents and starting materials were purchased from commercial sources and used without further purification unless otherwise stated. Dry DCM was obtained by distillation over CaH_2 prior to use. POPC was supplied by Genzyme. NMR titrations were performed by addition of aliquots of the putative anionic guest as the tetrabutylammonium (TBA) or tetraethylammonium (TEA) salt (0.15 M), in a solution of the receptor (0.01 M) in DMSO-d_6 to 0.01 M solution of the receptor. Chloride concentrations during transport experiments were determined using an Accumet or Cole-Parmer chloride selective electrode. Fluorescence spectra were recorded using a Varian Cary Eclipse Fluorescence Spectrophotometer. pH values were determined using an Eutech Instruments pH sensitive electrode.

Synthesis

The synthesis of each of these compounds has been reported elsewhere[1-7]. A general outline of the procedure used in this case is given below.

Tris(2-aminoethyl)amine (0.40 g, 2.73 mmol) was dissolved in dry DCM (20 mL) and 3 equivalents of the appropriate isocyanate or isothiocyanate in 20 mL dry DCM was added dropwise under N_2. The mixture was stirred under N_2 at room temperature overnight. Purification and characterizing data were as follows:

1,1',1''-(nitrilotris(ethane-2,1-diyl))tris(3-butylurea), 1[1,2,3]

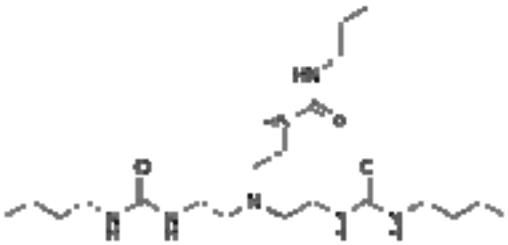

The gel-like precipitate was isolated by filtration and re-dissolved in a minimum volume of DCM. Recrystallization was induced by the dropwise addition of hexane to give compound **1** as a white solid.

Yield: 0.40 g (33%); ^{1}H NMR (300 MHz, DMSO-d_6): δ= 5.86 (br. s, 3H, urea NH), 5.79 (br.s, 3H, urea NH), 2.98 (m, 12H, overlapping CH_2 signals), 2.42 (m, 6H, CH_2), 1.29 (m, 12H, overlapping CH_2 signals), 0.86 (t, 9H, J= 6.6 Hz, CH_3); ^{13}C NMR (75 MHz, DMSO-d_6): δ= 155.3 (CO), 140.5 (aromatic CH), 128.6 (aromatic CH), 121.0 (aromatic CH), 117.7 (aromatic CH), 54.0 (CH_2), 37.5 (CH_2); LRMS(ESI+): *m/z*= 444.5 $[M + H]^+$, 466.5 $[M + Na]^+$; HRMS(ES): for $C_{21}H_{45}N_7O_3$ $[M + H]^+$ *m/z*= 444.3662 (calculated), 444.3657 (found); IR (film): ν= 3300 (urea NH stretching), 1630+ 1580 (carbonyl CO stretching); M_p= 160-162 °C.

1,1',1''-(nitrilotris(ethane-2,1-diyl))tris(3-phenylurea), 2[1,4,5]

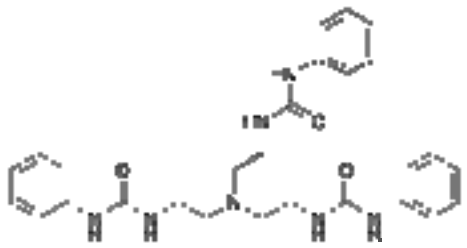

The solvent was removed under reduced pressure. The solid was re-dissolved in a minimum volume of DCM and recrystallization was induced by the dropwise addition of hexane to give compound **1** as a white solid.

Yield: 1.30 g (95%); ^{1}H NMR (300 MHz, DMSO-d_6): δ= 8.51 (s, 3H, urea NH), 7.37 (d, 6H, J= 8.3 Hz, aromatic CH), 7.19 (m, 6H, aromatic CH), 6.87 (m, 3H, aromatic CH), 6.18 (t, 3H, J= 5.1 Hz, urea NH), 3.18 (m, 6H, CH_2), 2.59 (t, 6H, J= 6.4 Hz, CH_2); ^{13}C NMR (75 MHz, DMSO-d_6): δ= 155.3 (CO), 140.5 (aromatic CH), 128.6 (aromatic CH), 121.0 (aromatic CH), 117.7 (aromatic CH), 34.0 (CH_2), 37.5 (CH_2); LRMS (ESI+): *m/z*= 504.4 $[M + H]^+$, 526.4 $[M + Na]^+$; HRMS(ES): for $C_{27}H_{33}N_7O_3$ $[M + H]^+$ *m/z*= 504.2723 (calculated), 504.2718 (found); IR (film): ν= 3310 (urea NH stretching, broad), 1680,1650 (carbonyl CO stretching); M_p= 195-197 °C

1,1',1''-(nitrilotris(ethane-2,1-diyl))tris(3-butylthiourea), 3[6,7]

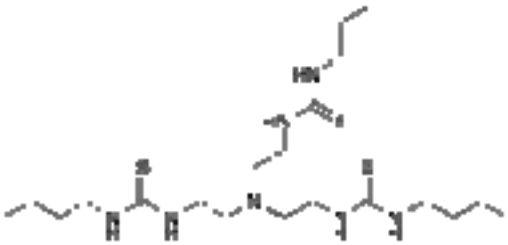

The solvent was removed under reduced pressure and the crude mixture was purified by column chromatography on silica-gel eluent 5% MeOH in DCM) and dried *in vacuo*. Compound **3** was isolated as a thick yellow oil.

Yield: 0.95 g (37%); ^{1}H NMR (300 MHz, DMSO-d_6): δ= 7.50 (br. s, 3H, urea NH), 7.20 (s, 3H, urea NH), 3.44 (br. m, overlaps with water signal, 6H, CH_2), 2.60 (t, 6H, J= 6.6 Hz, CH_2), 1.44 (m, 6H, CH_2), 1.27 (m, 6H, CH_2)m, 0.87 (t, 9H, J= 7.35 Hz, CH_3); ^{13}C NMR (75 MHz, DMSO-d_6): δ= 182.0 (CO), 52.6 (CH_2), 43.2 (CH_2), 41.5 (CH_2), 30.9 (CH_2), 19.6 (CH_2), 13.7 (CH_3); LRMS (ESI+): *m/z*= 492.4 $[M + H]^+$, 514.4 $[M + Na]^+$; HRMS (ES): for $C_{21}H_{45}N_7S_3$ $[M + H]^+$ *m/z*= 492.2977 (calculated), 492.2971 (found); IR (film): ν= 3260 (thiourea NH stretching), 3060 (thiourea NH stretching), 1540 (CS stretching).

1,1',1''-(nitrilotris(ethane-2,1-diyl))tris(3-phenylthiourea), 4[1]

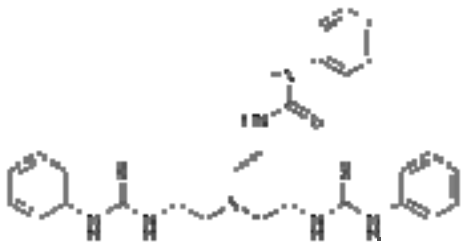

The solvent was removed under reduced pressure. The crude product was purified by column chromatography on silica-gel (eluent 2% MeOH in DCM). The solvent was removed under reduced pressure. The obtained product was refluxed overnight in hexane to remove all traces of DCM. The hexane was subsequently removed *in vacuo* to give compound **4** as a colourless oil which formed a white solid on standing (1.47 g, 98% yield).

Yield: 1.47 g (98%); ^{1}H NMR (300 MHz, DMSO-d_6): δ= 9.60 (s, 3H, thiourea NH), 7.62 (br. s, 3H, thiourea NH), 7.40-7.29 (m, 12H, overlapping aromatic CH), 7.10 (m, 3H, aromatic CH), 3.57 (m, 6H, CH_2), 2.72 (t, 6H, J= 6.6 Hz, CH_2); ^{13}C NMR (75 MHz, DMSO-d_6): δ= 180.2 (CO), 139.0 (aromatic CH), 128.7 (aromatic CH), 124.2 (aromatic CH), 123.2 (aromatic CH), 54.9 (CH_2), 52.1 (CH_2); LRMS(ESI+): *m/z*= 552.4 $[M + H]^+$, 574.3 $[M + Na]^+$; HRMS(ES): for $C_{27}H_{33}N_7S_3$ $[M + H]^+$ *m/z*= 552.2038 (calculated), 552.2027 (found); IR(film): ν= 3380 (thiourea NH stretching), 3320 (thiourea NH stretching), 1590 + 1530+ 1490 +1450 (CS stretching); M_p= 64-66 °C.

Vesicle Studies

Preparation of Vesicles

A lipid film of 1-palmitoyl-2-oleoyl-*sn*-glycero-3-phosphocholine (POPC) and cholesterol (0% or 30%) was formed from a chloroform solution under reduced pressure and dried under vacuum for at least 6 hours. The lipid film was rehydrated by vortexing with a metal chloride (MCl) salt solution (489 mM MCl, 5 mM phosphate buffer at pH 7.2). The lipid suspension was then subjected to seven freeze-thaw cycles and allowed to age for 30 min at room temperature before extruding 25 times through a 200 nm polycarbonate membrane. The resulting unilamellar vesicles were dialyzed against the external medium to remove unencapsulated MCl salts.

Chloride Transport Assays

Unilamellar POPC vesicles containing NaCl, prepared as described above, were suspended in 489 mM $NaNO_3$ or 162 mM Na_2SO_4 solution buffered to pH 7.2 with sodium phosphate salts. The lipid concentration per sample was 1 mM. A DMSO solution of the carrier molecule (10 mM) was added to start the experiment and the chloride efflux was monitored using a chloride sensitive electrode. At 5 min, the vesicles were lysed with 50 μl of polyoxyethylene(8)lauryl ether (0.232 mM in 7:1 water:DMSO v/v) and a total chloride reading was taken at 7 min. In the case of the external anion being

sulfate, the experiment was extended such that the vesicles were lysed at 20 min and total chloride reading taken at 22 min.

Bicarbonate Transport Assay (ISE)

Unilamellar POPC vesicles containing 489 mM NaCl solution buffered to pH 7.2 with 20 mM sodium phosphate salts, prepared as described above, were suspended in 162 mM Na_2SO_4 solution buffered to pH 7.2 with sodium phosphate salts. The lipid concentration per sample was 1 mM. A DMSO solution of the carrier molecule (10 mM) was added to start the experiment and chloride efflux was monitored using a chloride sensitive electrode. At 2 min, $NaHCO_3$ solution (1.2 M in 162 mM Na_2SO_4 buffered to pH 7.2 with 20 mM sodium phosphate salts) was added so that the outer solution contained 40 mM $NaHCO_3$. At 8 min, the vesicles were lysed with 50 μl of polyoxyethylene(8)lauryl ether (0.232 mM in 7:1 water:DMSO v/v) and a total chloride reading was taken at 10 min.

General Experimental for ^{13}C NMR Liposome Assays

^{13}C NMR spectra were recorded on a Bruker AVIII-600 operating at 150.92 MHz. Deuterated solvents were purchased from Cambridge Isotope Labs. Phospholipids used to prepare liposomes were purchased from Avanti Polar Lipids. High-pressure extrusion was performed on the Avanti mini-extruder using a 5.0 mm polycarbonate membrane. Dialysis was performed using a #2 Spectra/Por dialysis membrane. ^{13}C labeled sodium bicarbonate was purchased from Sigma/Isotec. All other chemicals were purchased from Sigma, Aldrich, Fisher, Fluka or Acros and used without further purification.

Preparation of Liposomes for ^{13}C NMR Anion Transport Assay

A stock solution of egg-yolk phosphatidylcholine (EYPC) in $CHCl_3$ (280 mg in 14 mL) was evaporated under reduced pressure to produce a thin film that was dried *in vacuo* overnight. The lipid film was hydrated with a 2 mL solution

containing 20 mM HEPES (pH 7.4) and 100 mM $NaH^{13}CO_3$ in a 9:1 H_2O/D_2O mixture. Freeze/thaw cycles were repeated at 6 times until no solids were visible. The frozen solution was warmed to 30-35 ^oC before each freeze cycle. The mixture was placed on a vortexer every 3 cycles for 30 s to facilitate hydration. The cloudy solution was extruded in 2 separate 1 mL batches through a 5.0 mm polycarbonate membrane 25 times. In order to exchange external $NaH^{13}CO_3$ with Na_2SO_4, this solution was placed in dialysis tubing and stirred in a 9:1 H_2O/D_2O solution containing of 20 mM HEPES and 75 mM Na_2SO_4 at pH 7.4 for 4 hr. Stock solutions of liposomes were stored in the refrigerator and used within 24 hr. for transport assays. Liposome stock solution concentration was determined assuming 90% retention of lipid throughout preparation process.

^{13}C NMR Anion Transport Assays

^{13}C NMR spectra were recorded on a Bruker AVIII-600 operating at 150.92 MHz, with chemical shifts reported in ppm. The instrument was locked on 9:1 H_2O/D_2O. Experimental conditions were: temperature, 27 °C; acquisition time, 0.93 s; spectrum width 35,211 Hz; relaxation delay, 0.2 s; number of scans, 196. For each experiment, an initial ^{13}C NMR spectrum of a 520 µL of the liposome solution was acquired. This solution consisted of EYPC liposomes containing 100 mM $NaH^{13}CO_3$ buffered to pH 7.4 with 20 mM HEPES, dispersed in 75 mM Na_2SO_4 buffered to pH 7.4 with 20 mM HEPES. A NaCl pulse followed, resulting in final extravesicular concentrations of 41 mM lipid and 50 mM NaCl. The ^{13}C NMR of this liposome mixture was taken, followed by the addition of a solution of **1-4** (in DMSO, 15 µL) or 15 µL of DMSO. Ligands **1-4** were added to give a 0.04 molar equiv. to lipid ratio. A ^{13}C NMR of the ligand containing mixture was acquired before and after the addition 3 µL of a solution of $MnCl_2$ (0.5 mM final Mn^{2+} concentration).

Additional vesicle experiments

Mobility Assays

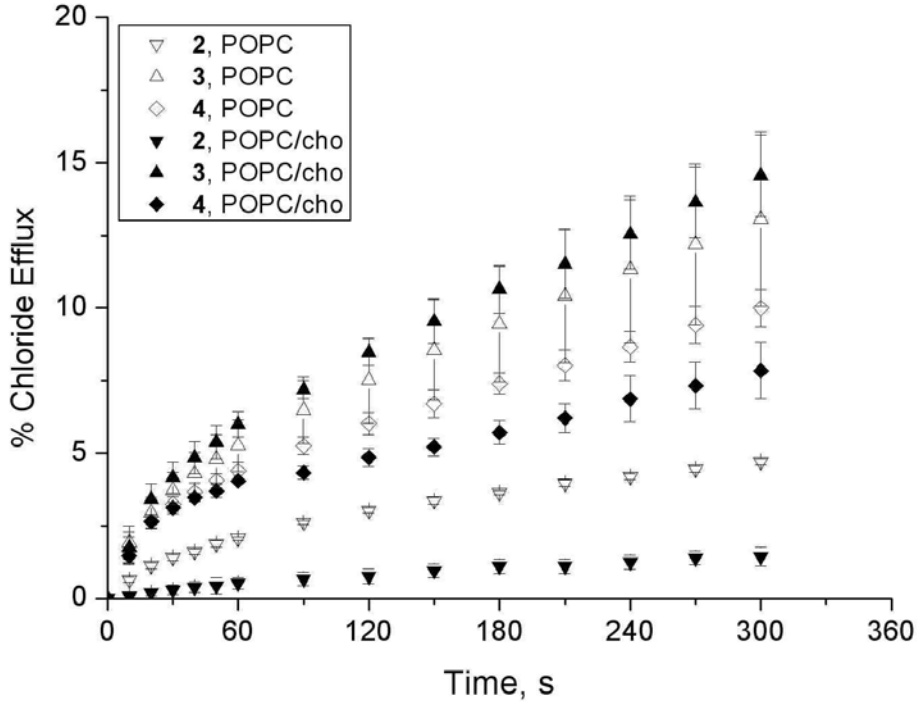

Figure S1 Chloride efflux promoted by 0.02 molar equiv compounds **2**, **3** and **4** from unilamellar POPC (open symbols) and POPC:cholesterol (70:30) (closed symbols) vesicles loaded with 489 mM NaCl buffered to pH 7.2 with 5 mM sodium phosphate salts. The vesicles were dispersed in 162 mM Na_2SO_4 buffered to pH 7.2 with 5 mM sodium phosphate salts. At the end of the experiment, detergent was added to lyse the vesicles and calibrate the ISE to 100% chloride efflux. Each point represents the average of three trials. Error bars represent the standard deviation.

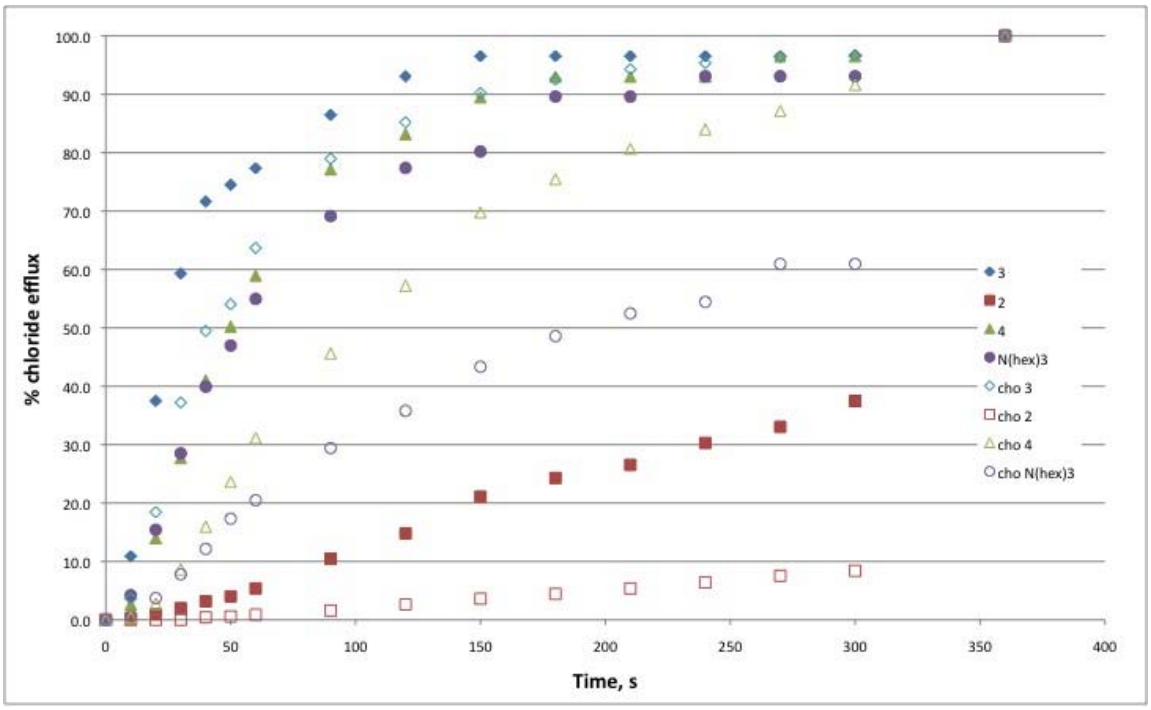

Figure S2 Chloride efflux promoted by 0.02 molar equiv compounds **2**, **3** and **4** from unilamellar POPC (open symbols) and POPC:cholesterol (70:30) (closed symbols) vesicles loaded with 489 mM NaCl buffered to pH 7.2 with 5 mM sodium phosphate salts. The vesicles were dispersed in 489 mM $NaNO_3$ buffered to pH 7.2 with 5 mM sodium phosphate salts. At the end of the experiment, detergent was added to lyse the vesicles and calibrate the ISE to 100% chloride efflux. Each point represents the average of three trials. Error bars represent the standard deviation.

Cation dependence

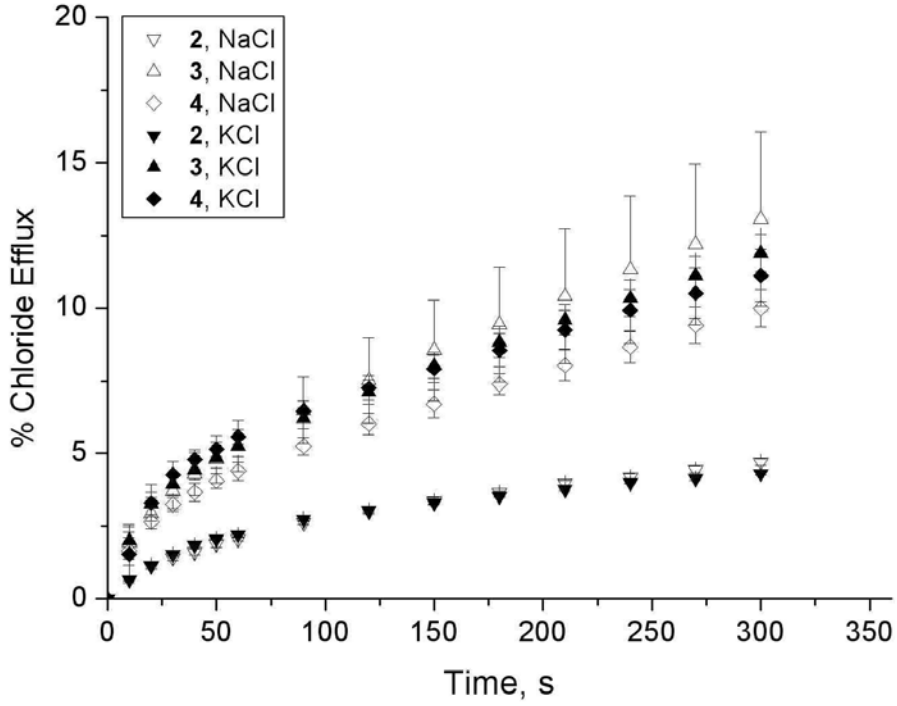

Figure S3 Chloride efflux promoted by 0.02 molar equiv receptors **2**, **3** and **4** from unilamellar POPC vesicles loaded with 489 mM MCl buffered to pH 7.2 with M^+ phosphate salts. M= Na (open symbols) or K (closed symbols). The vesicles were dispersed in 162 mM M_2SO_4 buffered to pH 7.2 with M^+ phosphate salts. At the end of the experiment, detergent was added to lyse the vesicles and calibrate the ISE to 100% chloride release. Each point represents the average of three trials. Error bars represent the standard deviation.

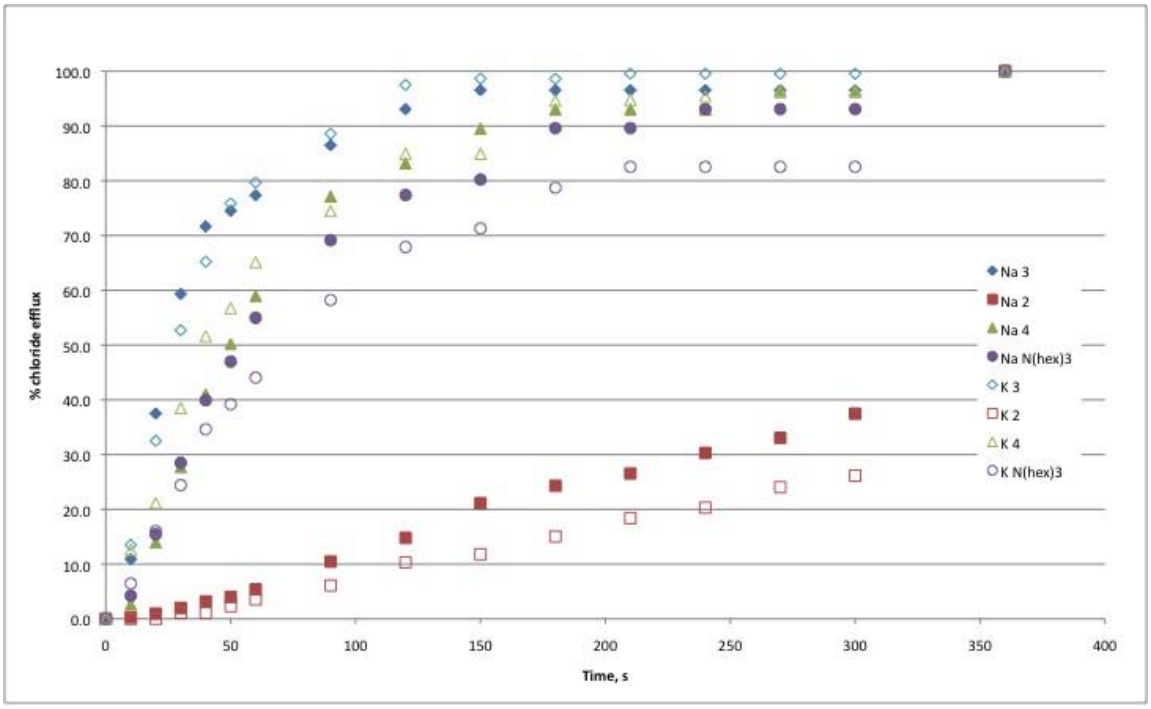

Figure S4 Chloride efflux promoted by 0.02 molar equiv receptors **2**, **3** and **4** from unilamellar POPC vesicles loaded with 489 mM MCl buffered to pH 7.2 with M^+ phosphate salts. M= Na (open symbols) or K (closed symbols). The vesicles were dispersed in 489 mM MNO_3 buffered to pH 7.2 with M^+ phosphate salts. At the end of the experiment, detergent was added to lyse the vesicles and calibrate the ISE to 100% chloride release. Each point represents the average of three trials. Error bars represent the standard deviation.

pH gradient

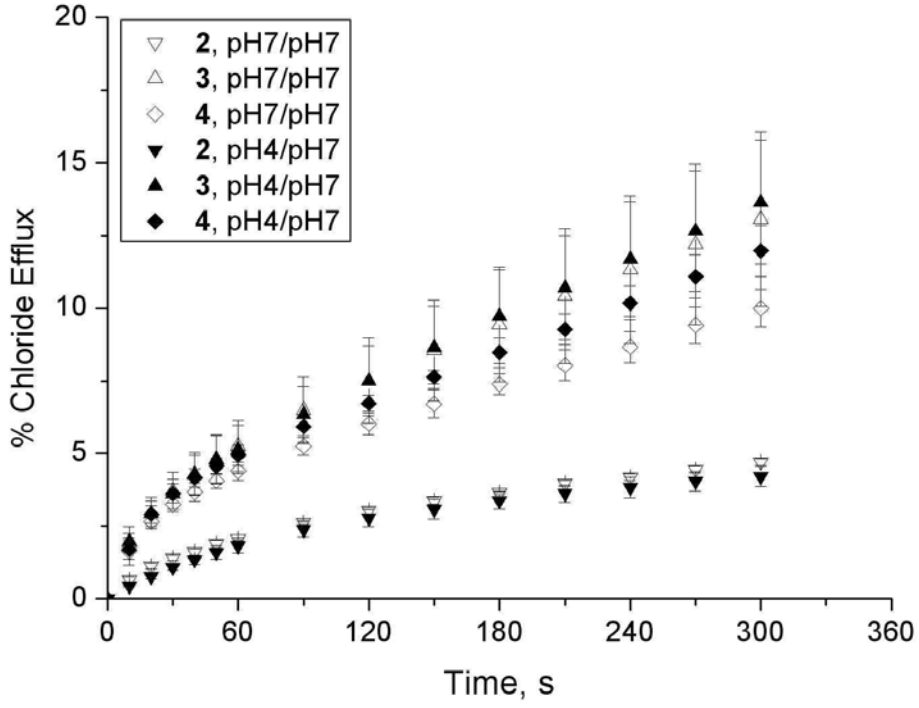

Figure S5 Chloride efflux promoted by 0.02 molar equiv receptors **2**, **3** and **4** from unilamellar POPC vesicles loaded with 489 mM NaCl buffered with sodium phosphate salts to either pH 7.2 (open symbols) or pH 4.0 (closed symbols). The vesicles were dispersed in 162 mM Na_2SO_4 buffered to pH 7.2 with sodium phosphate salts. At the end of the experiment, detergent was added to lyse the vesicles and calibrate the ISE to 100% chloride release. Each point represents the average of three trials.

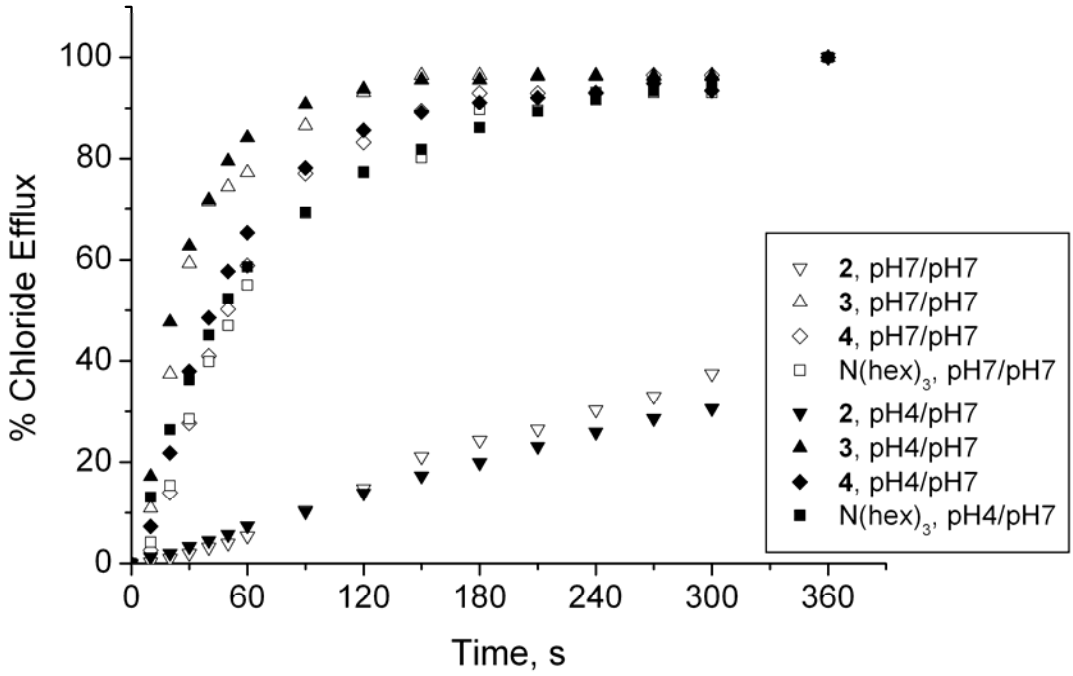

Figure S6 Chloride efflux promoted by 0.02 molar equiv receptors **2**, **3**, **4** or trihexylamine from unilamellar POPC vesicles loaded with 489 mM NaCl buffered with sodium phosphate salts to either pH 7.2 (open symbols) or pH 4.0 (closed symbols). The vesicles were dispersed in 489 mM $NaNO_3$ buffered to pH 7.2 with sodium phosphate salts. At the end of the experiment, detergent was added to lyse the vesicles and calibrate the ISE to 100% chloride release. Each point represents the average of three trials.

Concentration dependence

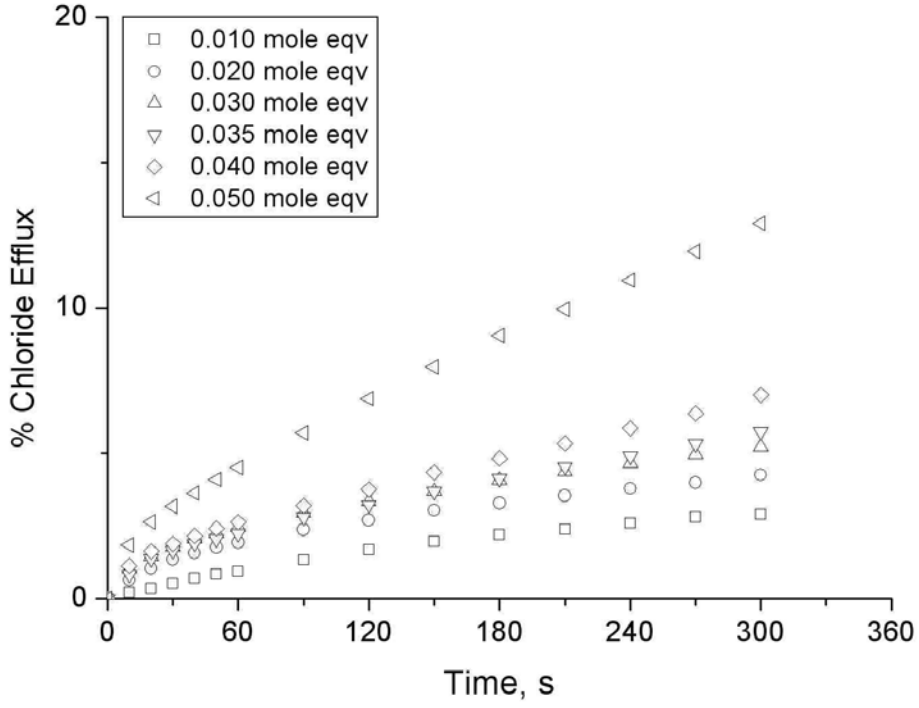

Figure S7 Chloride efflux promoted by various molar equiv of receptor **2** from unilamellar POPC vesicles loaded with 489 mM NaCl buffered to pH 7.2 with sodium phosphate salts. The vesicles were dispersed in 162 mM Na_sSO_4 buffered to pH 7.2 with sodium phosphate salts. At the end of the experiment, detergent was added to lyse the vesicles and calibrate the ISE to 100% chloride release. Each point represents the average of three trials.

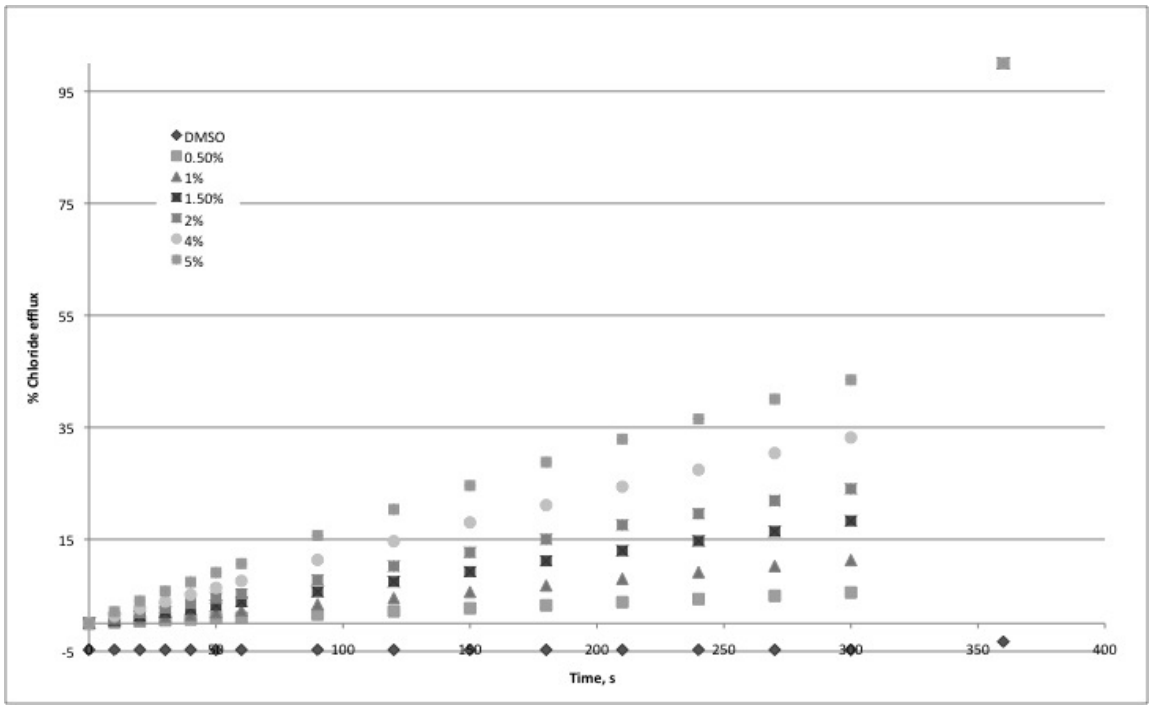

Figure S8 Chloride efflux promoted by various molar equiv of receptor **2** from unilamellar POPC vesicles loaded with 489 mM NaCl buffered to pH 7.2 with sodium phosphate salts. The vesicles were dispersed in 489 mM $NaNO_3$ buffered to pH 7.2 with sodium phosphate salts. At the end of the experiment, detergent was added to lyse the vesicles and calibrate the ISE to 100% chloride release. Each point represents the average of three trials.

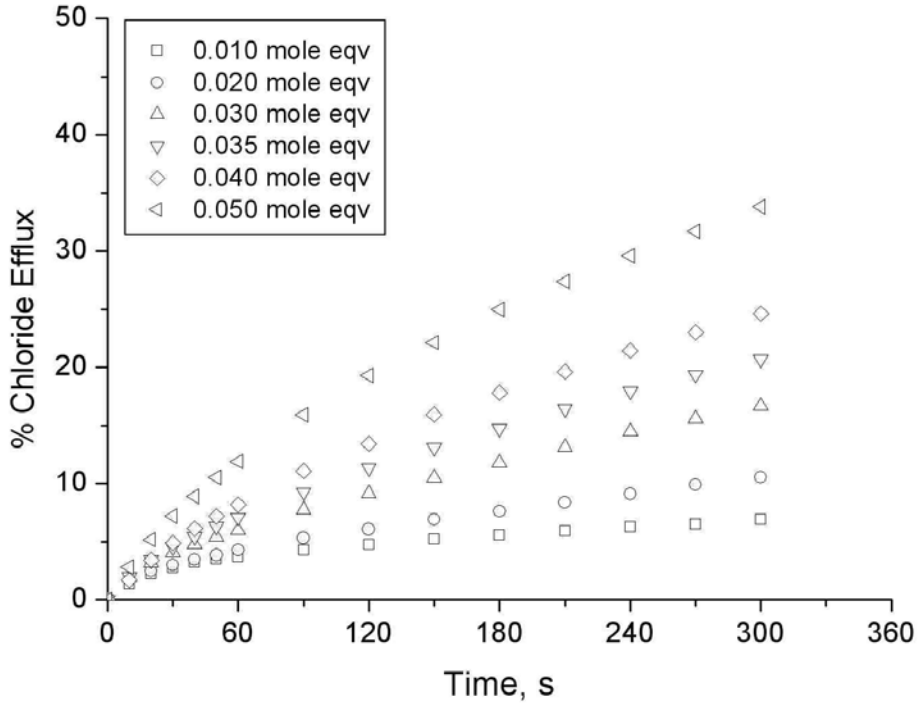

Figure S9 Chloride efflux promoted by various molar equiv receptor **3** from unilamellar POPC vesicles loaded with 489 mM NaCl buffered to pH 7.2 with sodium phosphate salts. The vesicles were dispersed in 162 mM Na_2SO_4 buffered to pH 7.2 with sodium phosphate salts. At the end of the experiment the vesicles detergent was added to lyse the vesicles and calibrate the ISE to 100% chloride release. Each point represents the average of 3 trials.

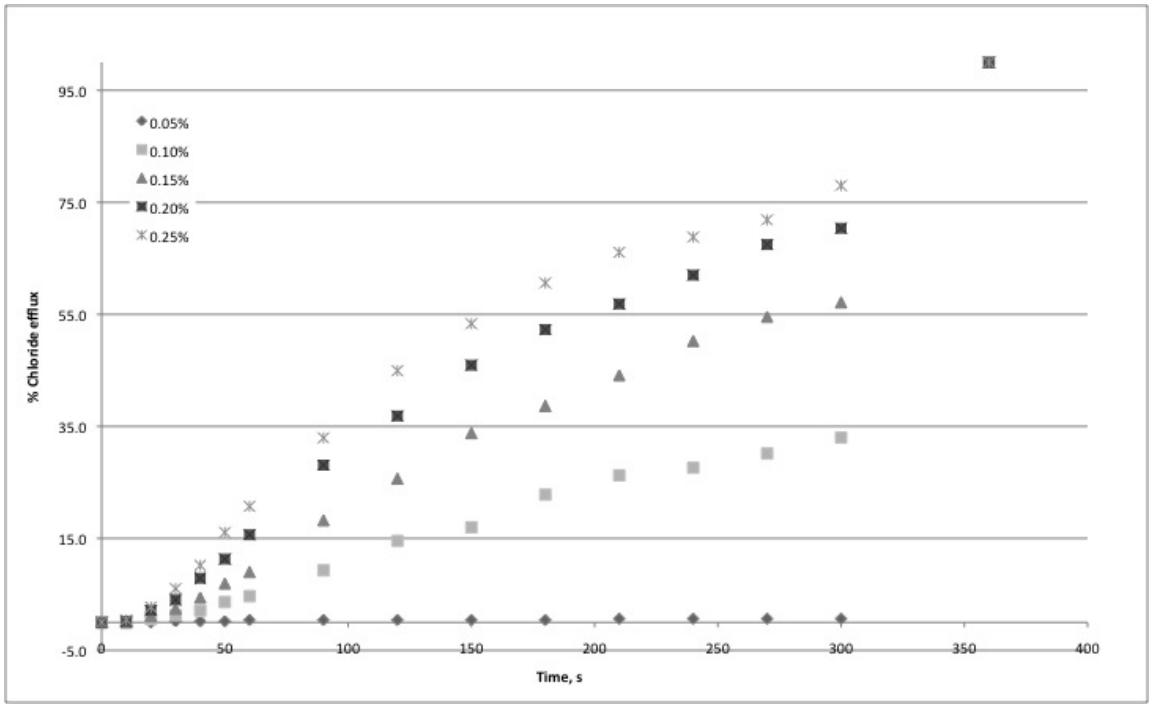

Figure S10 Chloride efflux promoted by various molar equiv of receptor **3** from unilamellar POPC vesicles loaded with 489 mM NaCl buffered to pH 7.2 with sodium phosphate salts. The vesicles were dispersed in 489 mM $NaNO_3$ buffered to pH 7.2 with sodium phosphate salts. At the end of the experiment, detergent was added to lyse the vesicles and calibrate the ISE to 100% chloride release. Each point represents the average of three trials.

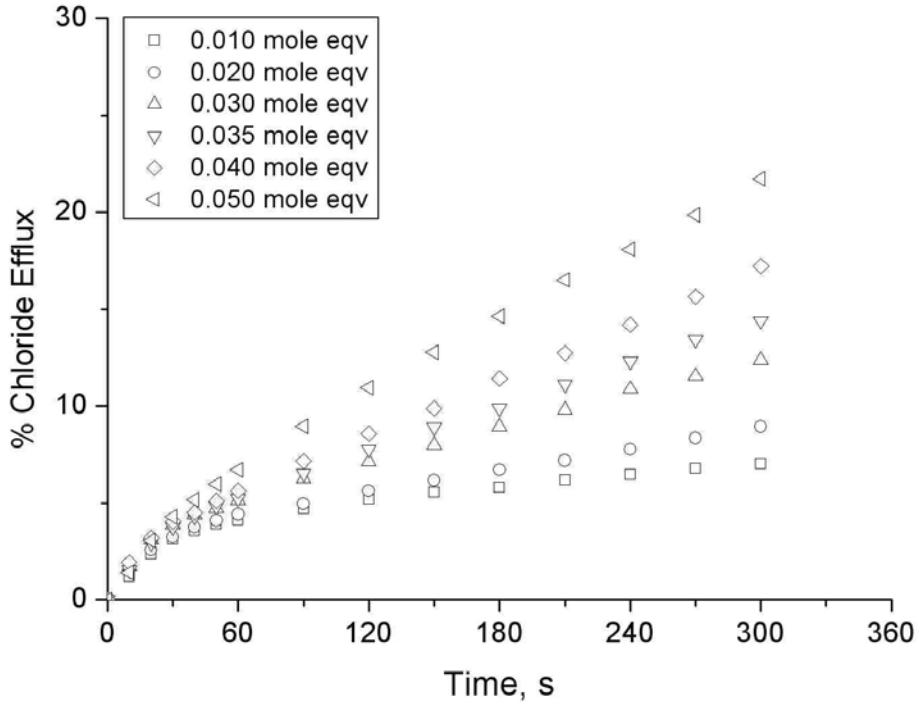

Figure S11 Chloride efflux promoted by various molar equiv receptor **4** from unilamellar POPC vesicles loaded with 489 mM NaCl buffered to pH 7.2 with sodium phosphate salts. The vesicles were dispersed in 162 mM Na_2SO_4 buffered to pH 7.2 with sodium phosphate salts. At the end of the experiment the vesicles detergent was added to lyse the vesicles and calibrate the ISE to 100% chloride release. Each point represents the average of 3 trials.

Discussion

We studied the release of chloride from vesicles containing 489 mM NaCl suspended in 167 mM Na_2SO_4 solution buffered to pH 7.2 over a longer time period (see ESI) in the presence of 4% molar carrier to lipid. These studies show that compounds **3** and **4** release chloride from the vesicles with approximately 50% of the chloride released over 1200 s. Compound **2** showed weaker transport activity whilst trihexylamine and compound **1** did not show any significant release of chloride under these conditions. A control experiment in which DMSO was added to the suspension of vesicles resulted in no release of chloride, evidence that addition of DMSO does not disrupt the structure of the vesicles in solution. HPTS assays conduced at 4% carrier loadings for compounds **2** – **4** show the same initial internal alkalinization as was observed in the Cl^-/NO_3^- systems (due to HCl co-transport) but no corresponding drift back of the internal pH (presumably as sulfate is too hydrophilic to be transported through the membrane by **2**-**4**) – for details see below.

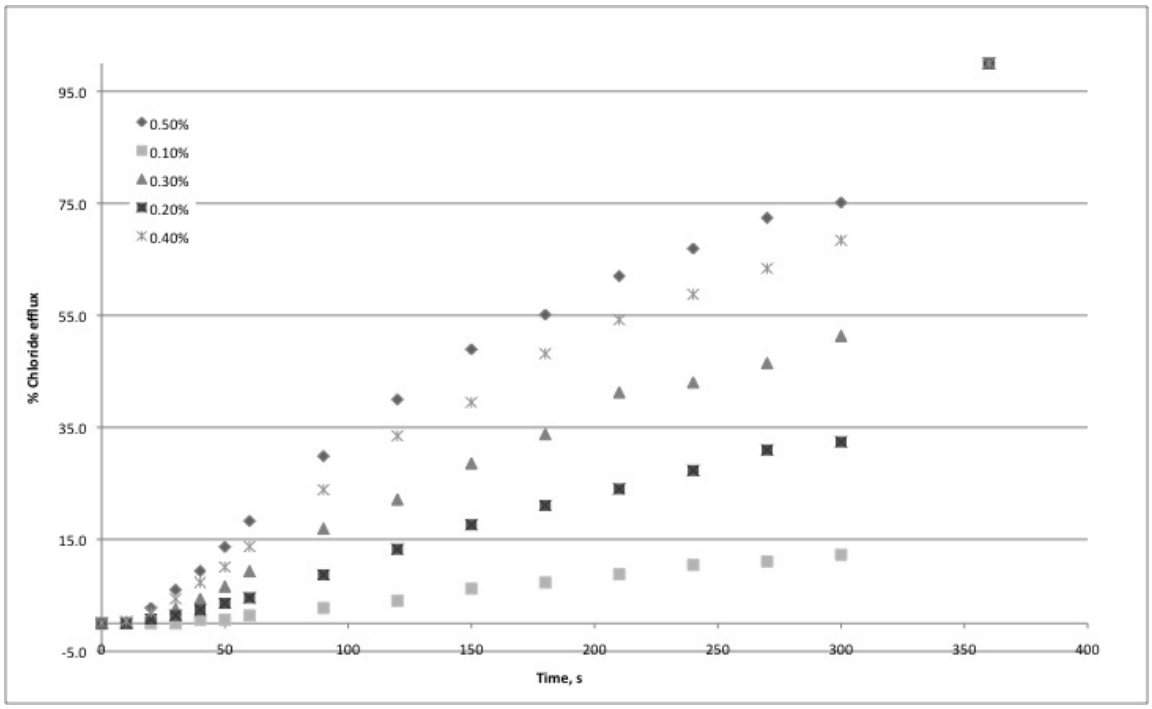

Figure S12 Chloride efflux promoted by various molar equiv of receptor **4** from unilamellar POPC vesicles loaded with 489 mM NaCl buffered to pH 7.2 with sodium phosphate salts. The vesicles were dispersed in 489 mM $NaNO_3$ buffered to pH 7.2 with sodium phosphate salts. At the end of the experiment, detergent was added to lyse the vesicles and calibrate the ISE to 100% chloride release. Each point represents the average of three trials.

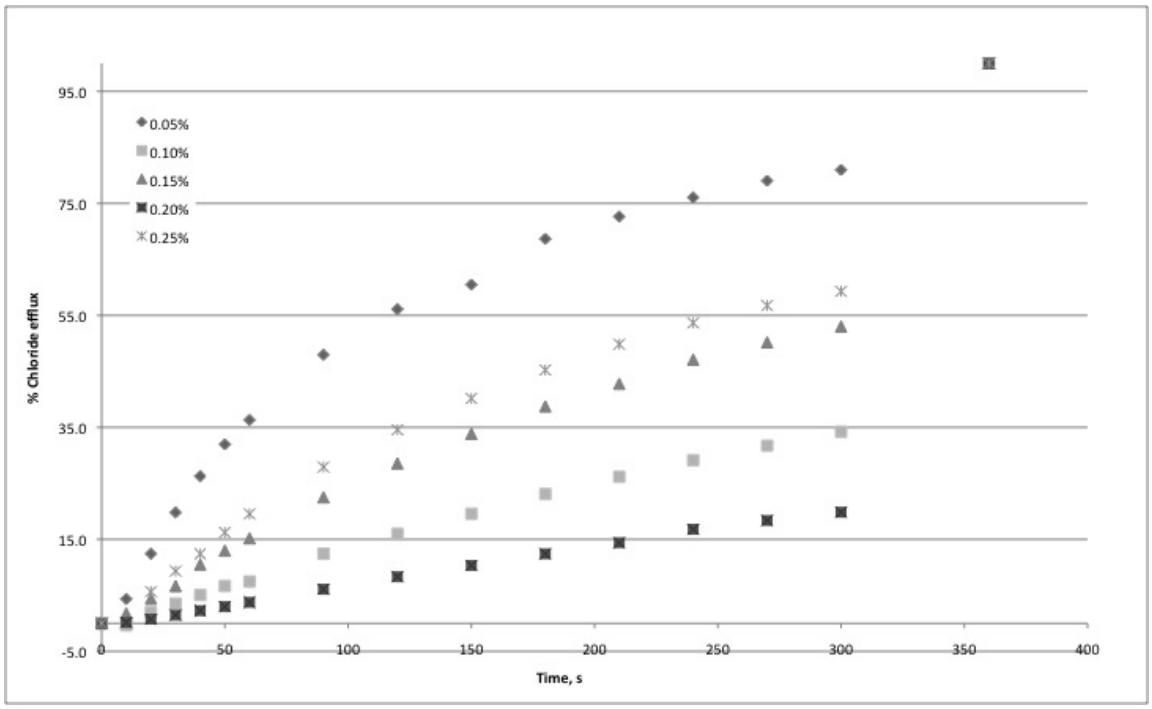

Figure S13 Chloride efflux promoted by various molar equiv of $N(hex)_3$ from unilamellar POPC vesicles loaded with 489 mM NaCl buffered to pH 7.2 with sodium phosphate salts. The vesicles were dispersed in 489 mM $NaNO_3$ buffered to pH 7.2 with sodium phosphate salts. At the end of the experiment, detergent was added to lyse the vesicles and calibrate the ISE to 100% chloride release. Each point represents the average of three trials.

Hill Analysis

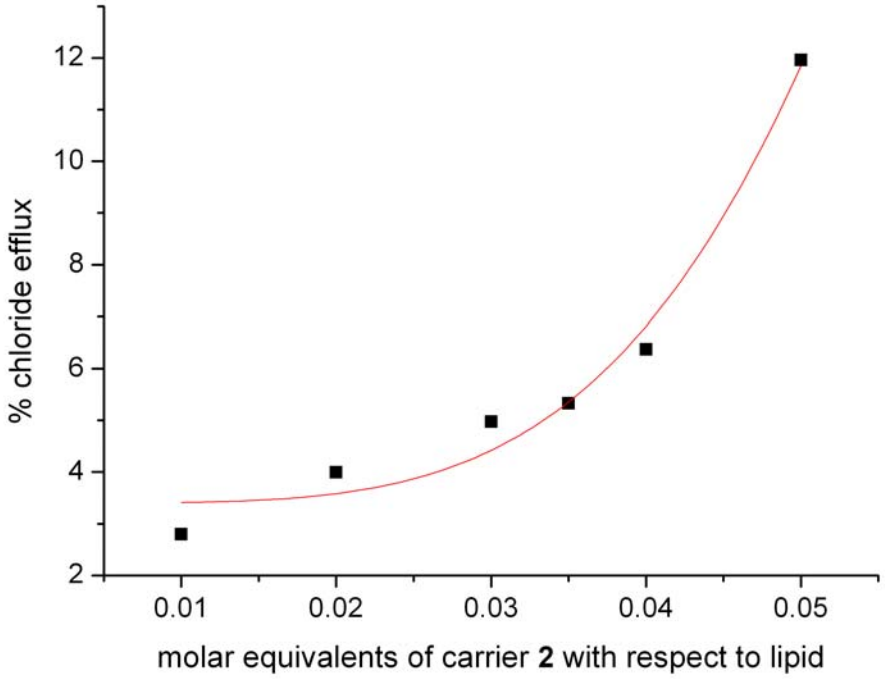

Figure S14 Hill plot for chloride release mediated by receptor **2** from unilamellar POPC vesicles loaded with 489 mM NaCl buffered to pH 7.2 with sodium phosphate salts. The vesicles were dispersed in 162 mM Na_2SO_4 buffered to pH 7.2 with 5 mM sodium phosphate salts. Chloride efflux was measured at 270 s.

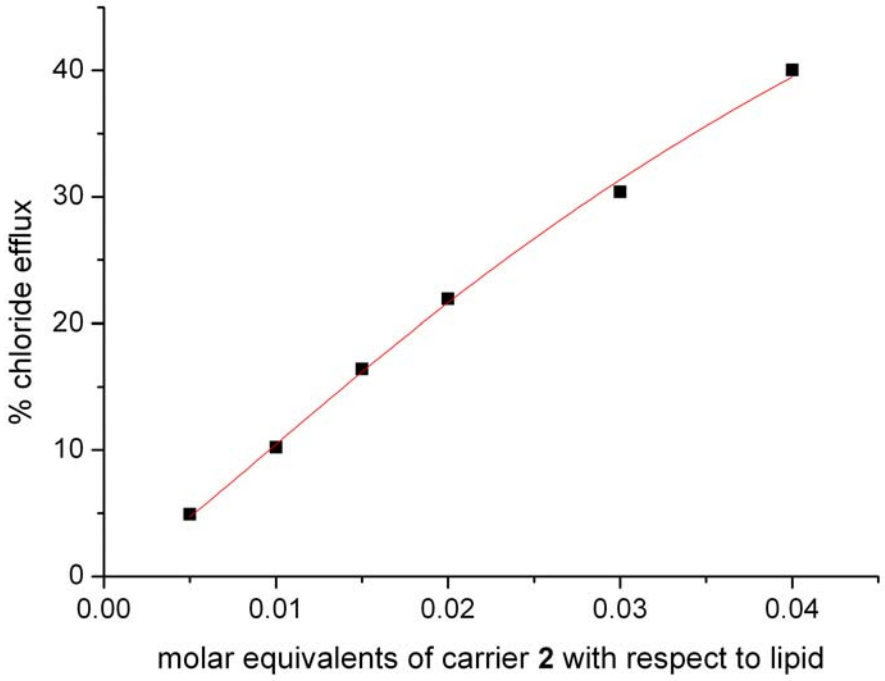

Figure S15 Hill plot for chloride release mediated by receptor **2** from unilamellar POPC vesicles loaded with 489 mM NaCl buffered to pH 7.2 with sodium phosphate salts. The vesicles were dispersed in 489 mM $NaNO_3$ buffered to pH 7.2 with 5 mM sodium phosphate salts. Chloride efflux was measured at 270 s.

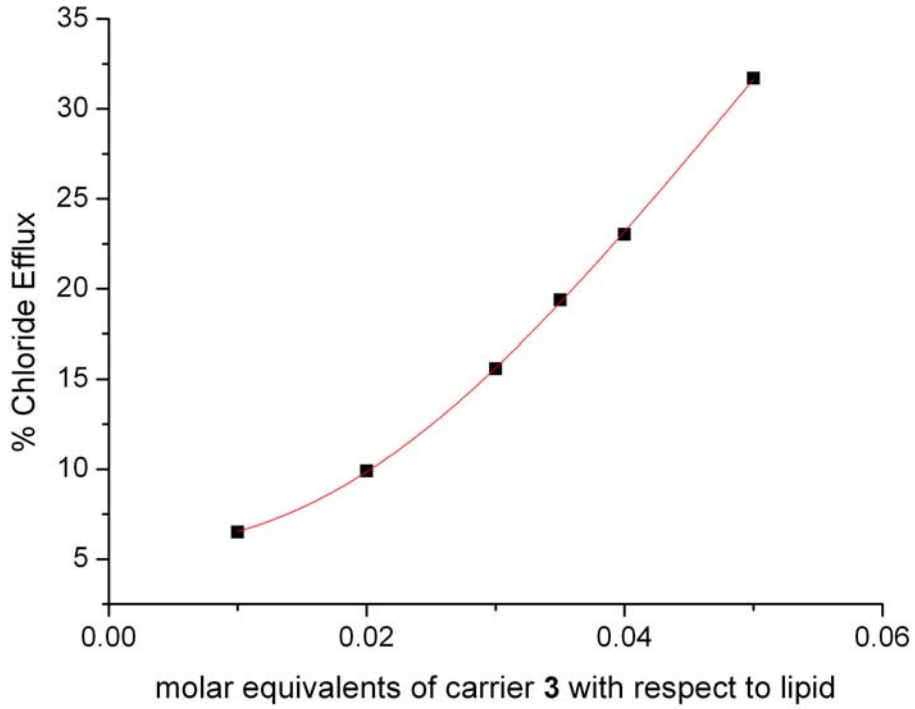

Figure S16 Hill plot for chloride release mediated by receptor **3** from unilamellar POPC vesicles loaded with 489 mM NaCl buffered to pH 7.2 with sodium phosphate salts. The vesicles were dispersed in 162 mM Na_2SO_4 buffered to pH 7.2 with 5 mM sodium phosphate salts. Chloride efflux was measured at 270 s.

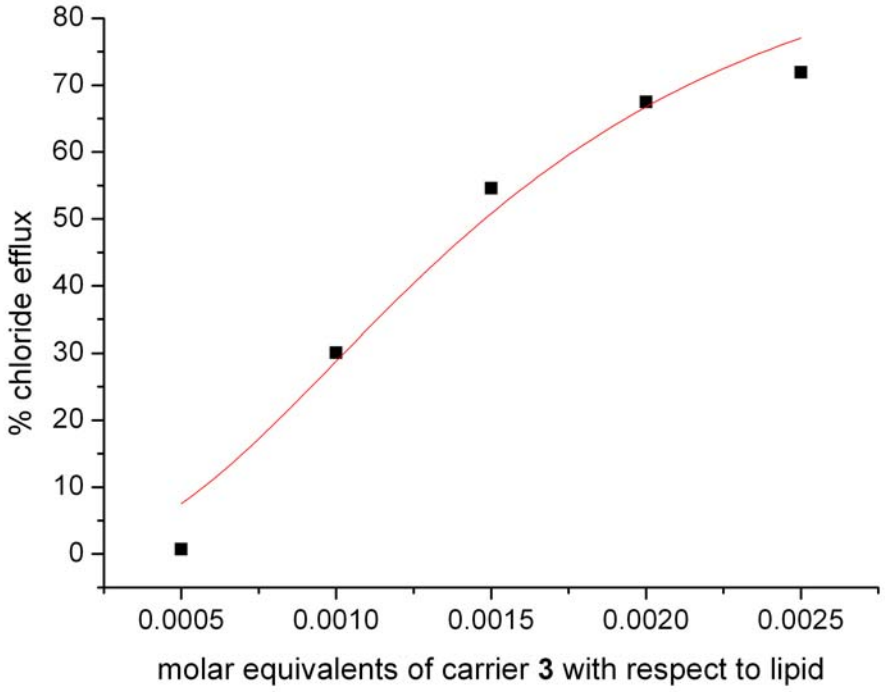

Figure S17 Hill plot for chloride release mediated by receptor **3** from unilamellar POPC vesicles loaded with 489 mM NaCl buffered to pH 7.2 with sodium phosphate salts. The vesicles were dispersed in 489 mM $NaNO_3$ buffered to pH 7.2 with 5 mM sodium phosphate salts. Chloride efflux was measured at 270 s.

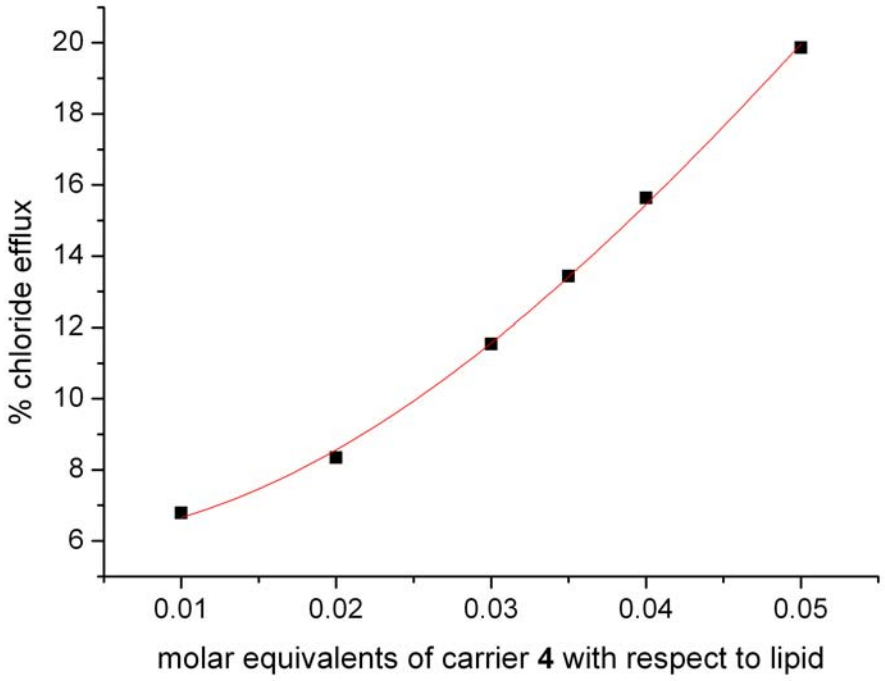

Figure S18 Hill plot for chloride release mediated by receptor **4** from unilamellar POPC vesicles loaded with 489 mM NaCl buffered to pH 7.2 with sodium phosphate salts. The vesicles were dispersed in 162 mM Na_2SO_4 buffered to pH 7.2 with 5 mM sodium phosphate salts. Chloride efflux was measured at 270 s.

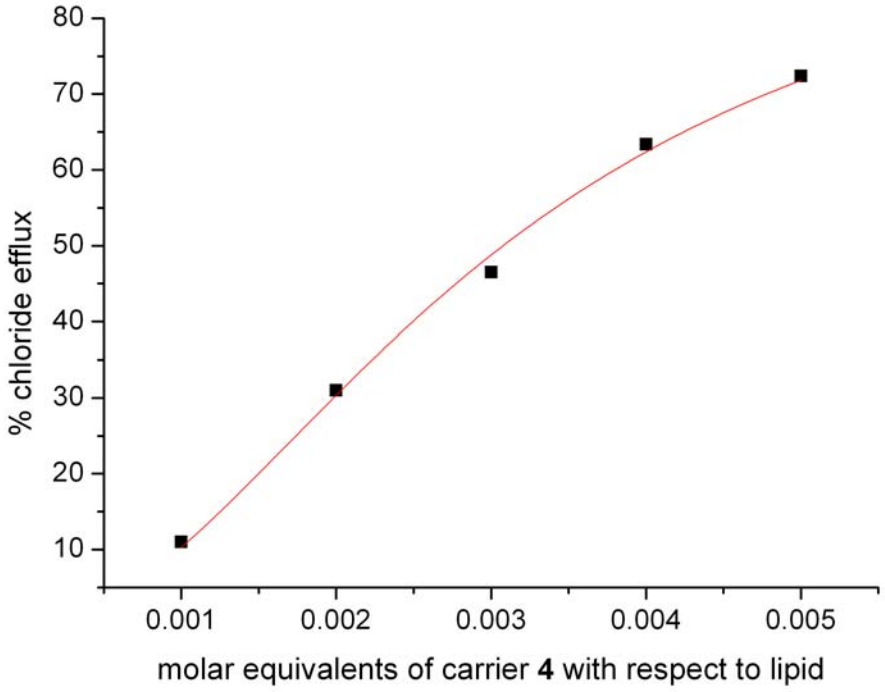

Figure S19 Hill plot for chloride release mediated by receptor **4** from unilamellar POPC vesicles loaded with 489 mM NaCl buffered to pH 7.2 with sodium phosphate salts. The vesicles were dispersed in 489 mM $NaNO_3$ buffered to pH 7.2 with 5 mM sodium phosphate salts. Chloride efflux was measured at 270 s.

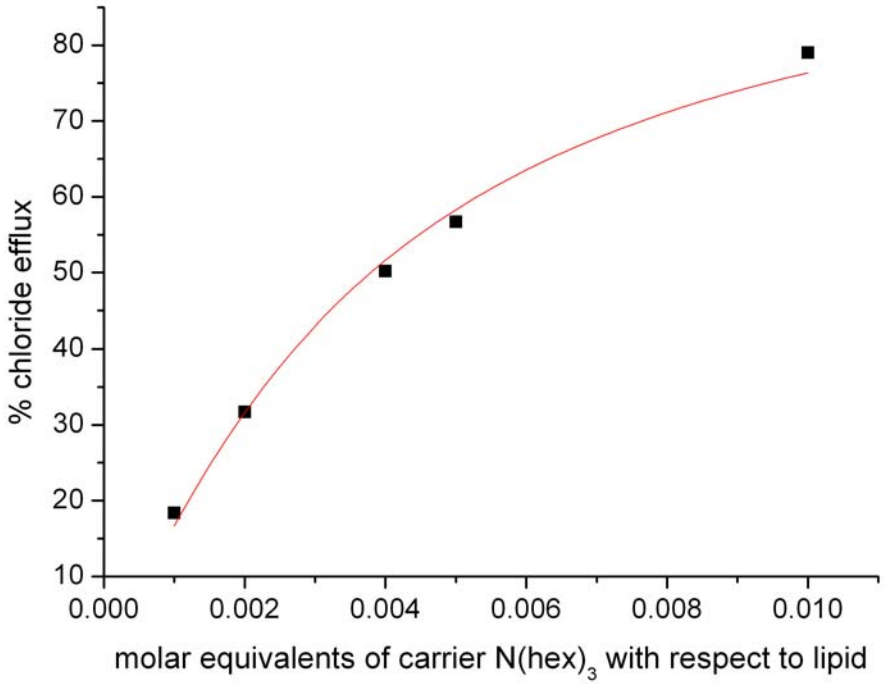

Figure S20 Hill plot for chloride release mediated by $N(hex)_3$ from unilamellar POPC vesicles loaded with 489 mM NaCl buffered to pH 7.2 with sodium phosphate salts. The vesicles were dispersed in 489 mM $NaNO_3$ buffered to pH 7.2 with 5 mM sodium phosphate salts. Chloride efflux was measured at 270 s.

System	Figure number	Start	End	k	n	EC_{50} at 270s (M)
2 Cl^-/SO_4^{2-}	S14	3.4 ± 0.5	100	0.08623 ±0.00884	4.30 ±0.81	0.084
3 Cl^-/SO_4^{2-}	S16	5.6± 0.2	100	0.07628 ±5e-4	2.28 ±0.04	0.024
4 Cl^-/SO_4^{2-}	S18	6.0 ± 0.3	100	0.120 ±0.005	2.00 ±0.09	0.11
$N(hexyl)_3$ Cl^-/NO_3^-	S20	0	100	0.00379 ±1.5e-4	1.21 ±0.07	0.0038
2 Cl^-/NO_3^-	S15	0	100	0.0564 ±0.0013	1.24 ±0.03	0.056
3 Cl^-/NO_3^-	S17	0	100	0.00148 ±8.2e-5	2.3 ±0.3	0.0015
4 Cl^-/NO_3^-	S19	0	100	0.00308 ±5.5e-5	1.9 ±0.09	0.0031

Table S1 Summary of data from Hill analysis

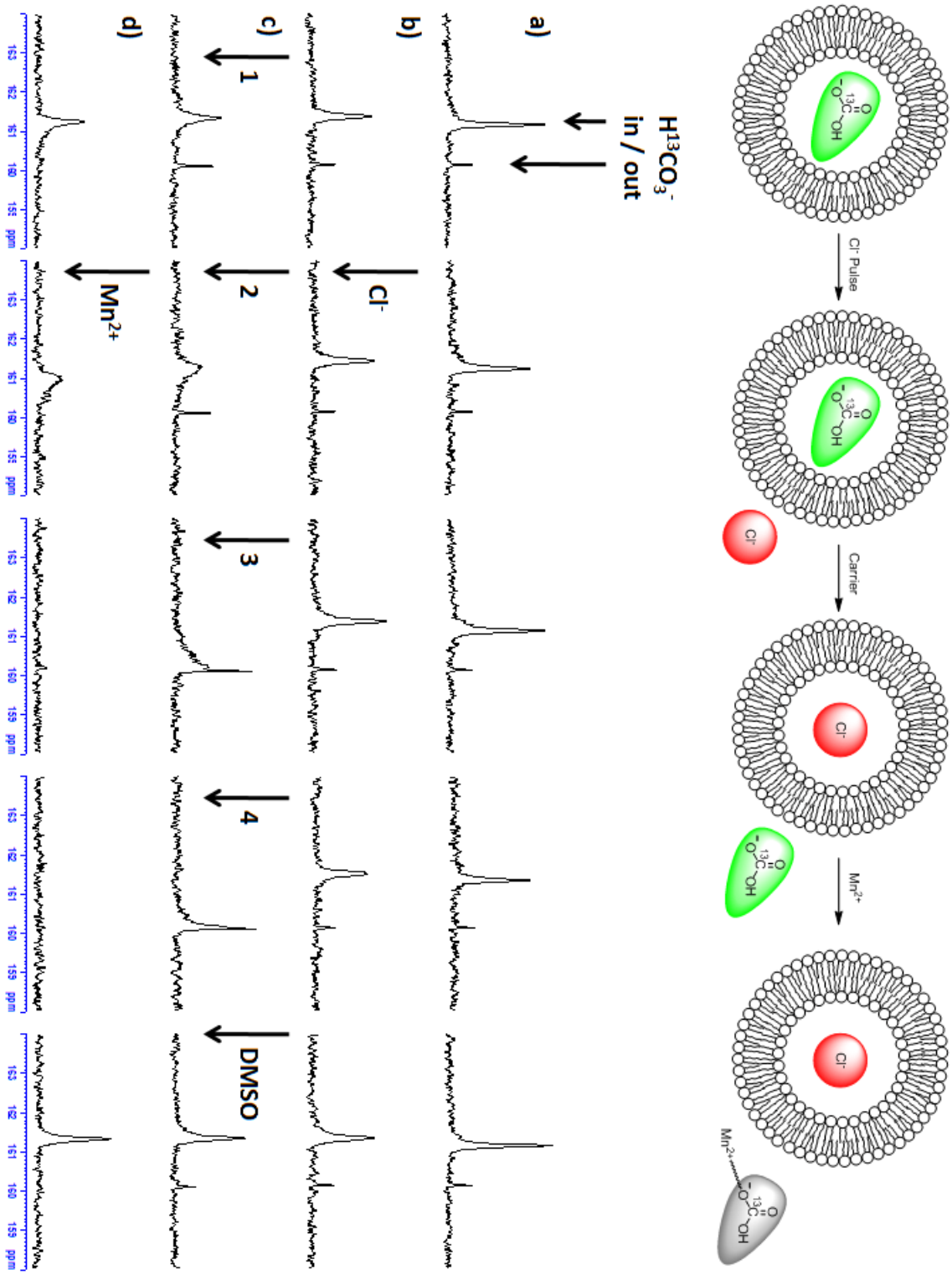

Figure S21. ^{13}C NMR liposome experiments following exchange of $H^{13}CO_3^-$ for Cl^- promoted by 0.04 molar equiv. of receptors **1-4**. a) before and b) after addition of a 50 mM NaCl pulse to EYPC vesicles containing 100 mM $NaH^{13}CO_3$ buffered to pH 7.4 with 20 mM HEPES, dispersed in 75 mM Na_2SO_4 buffered to pH 7.4 with 20 mM HEPES; c) following addition of **1**-**4** and DMSO; d) following addition of 0.5 mM $MnCl_2$, a paramagnetic line broadening agent that only affects external bicarbonate.

Fluorescence transport studies [8]

Unilamellar POPC vesicles were prepared as previously described containing 1 mM 8 - Hydroxypyrene - 1,3,6 - trisulfonic acid, trisodium salt (HPTS) and 500 mM NaCl buffered to pH 6.9 with sodium phosphate salts. In place of dialysis, the vesicles were subjected to size exclusion chromatography over Sephadex G50 eluting with 500 mM NaCl buffered to pH 6.9 with sodium phosphate salts in order to remove un-encapsulated HPTS. The lipid was diluted to 1 mM concentration using the required external eluent; either 489 mM $NaNO_3$ or 167 mM Na_2SO_4, both buffered to pH 6.9 with sodium phosphate salts. The sample size was 3 ml. Fluorescence measurements were initiated and a DMSO solution of the carrier (10 mM) was added after 10 s to start the experiment. The change in intravesicular pH was monitored by tracking the relative emission intensities at 510 nm due to excitation at 460 nm. and 403 nm. These excitation wavelengths correspond to the basic and acidic forms of HPTS respectively.[9,10] At 7 min, the vesicles were lysed with 30 μl of polyoxyethylene(8)lauryl ether (0.232 mM in 7:1 water:DMSO v/v).

The ratio I_1/I_0 was calibrated to pH as follows. The original 1 mM HPTS solution in 500 mM NaCl with 5 mM sodium phosphate salts was diluted to achieve the same fluorescence intensity as observed in the ion transport assay and was calculated to be 0.000002 M in HPTS. The fluorescence of HPTS dye in this solution containing 500 mM NaCl with 5 mM sodium phosphate salts was measured as a function of pH. The dependence of I_1/I_0 and $\log(I_1/I_0)$ on pH is shown below. I_1 and I_0 refer to the intensity of fluorescence emissions at 510 nm due to 460 nm (basic form of HPTS) and 403 nm (acidic form of HPTS) respectively.[9] The data was fitted to the following equation using Origin:

$$pH= -1/1.796*(\ln(4.2055/[I_1/I_0]-1))+7.6142$$

The results of the transport experiments and the calibration curves are shown below.

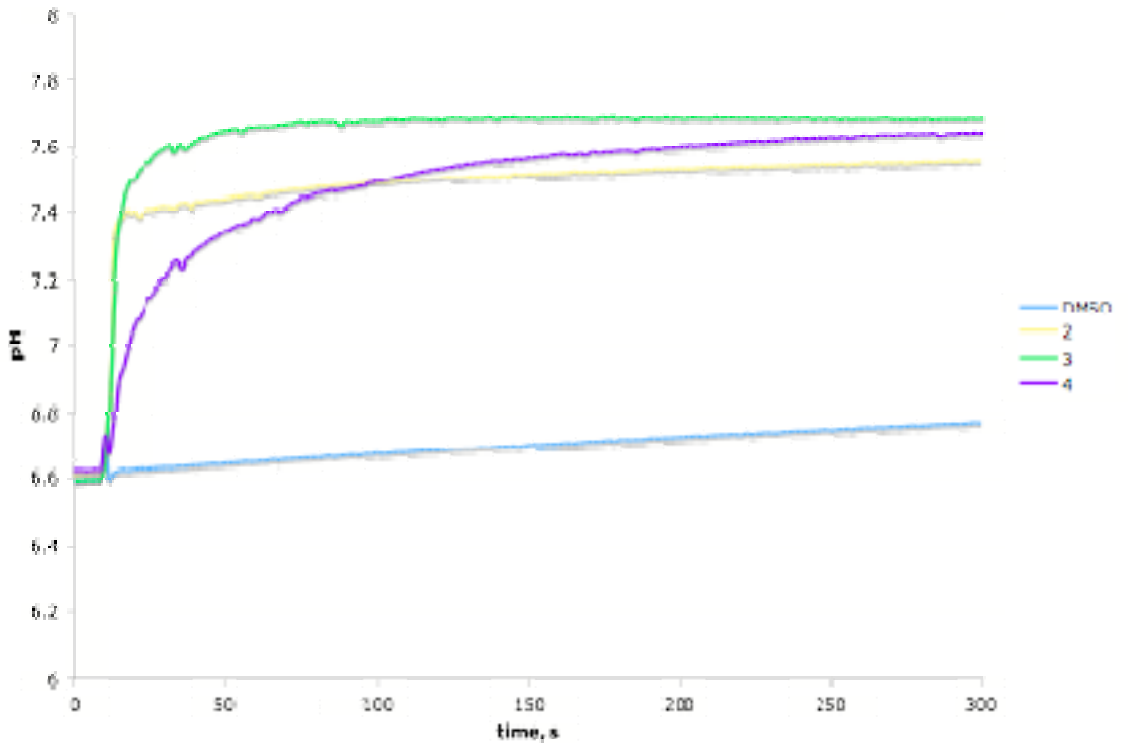

Figure S22 Change in intravesicular pH promoted by 0.04 molar equiv of receptors **2**-**4** from unilamellar POPC vesicles loaded with 500 mM NaCl and 1 mM HPTS buffered to pH 6.9 with sodium phosphate salts. The vesicles were dispersed in 167 mM Na_2SO_4 buffered to pH 6.9 with 5 mM sodium phosphate salts. At the end of the experiment, detergent was added to lyse the vesicles. Each point represents the average of three trials

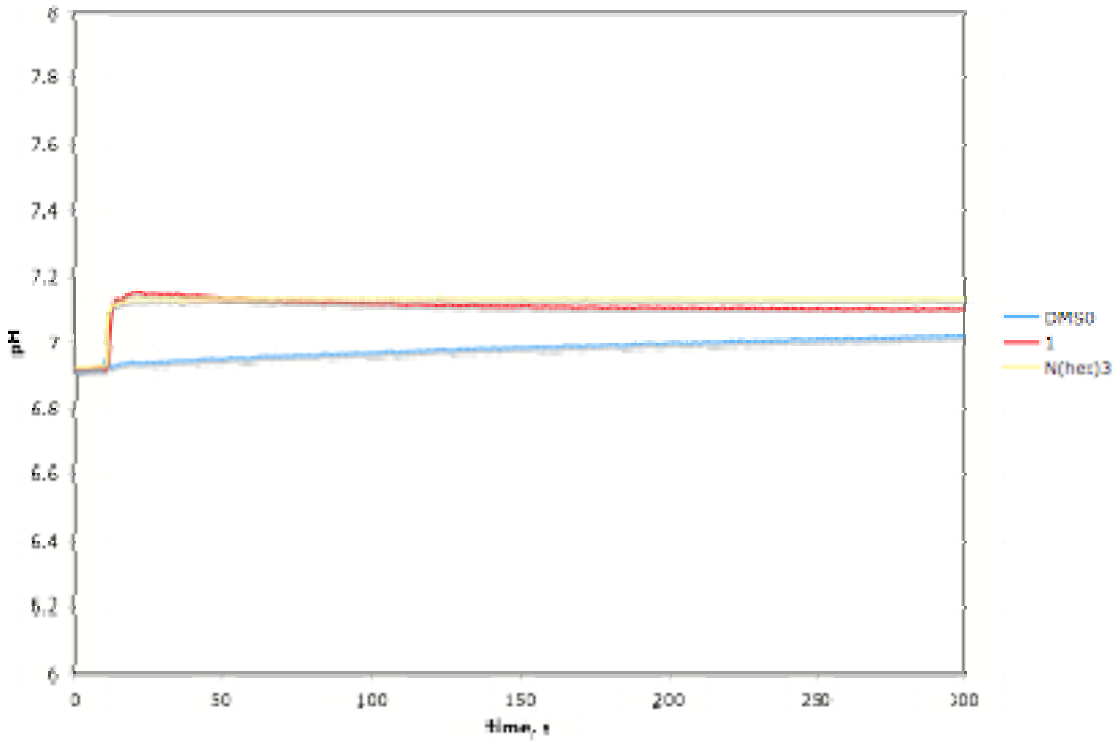

Figure S23 Change in intravesicular pH promoted by 0.04 molar equiv of receptor **1** and trihexylamine from unilamellar POPC vesicles loaded with 500 mM NaCl and 1 mM HPTS buffered to pH 6.9 with sodium phosphate salts. The vesicles were dispersed in 167 mM Na_2SO_4 buffered to pH 6.9 with 5 mM sodium phosphate salts. At the end of the experiment, detergent was added to lyse the vesicles. Each point represents the average of three trials

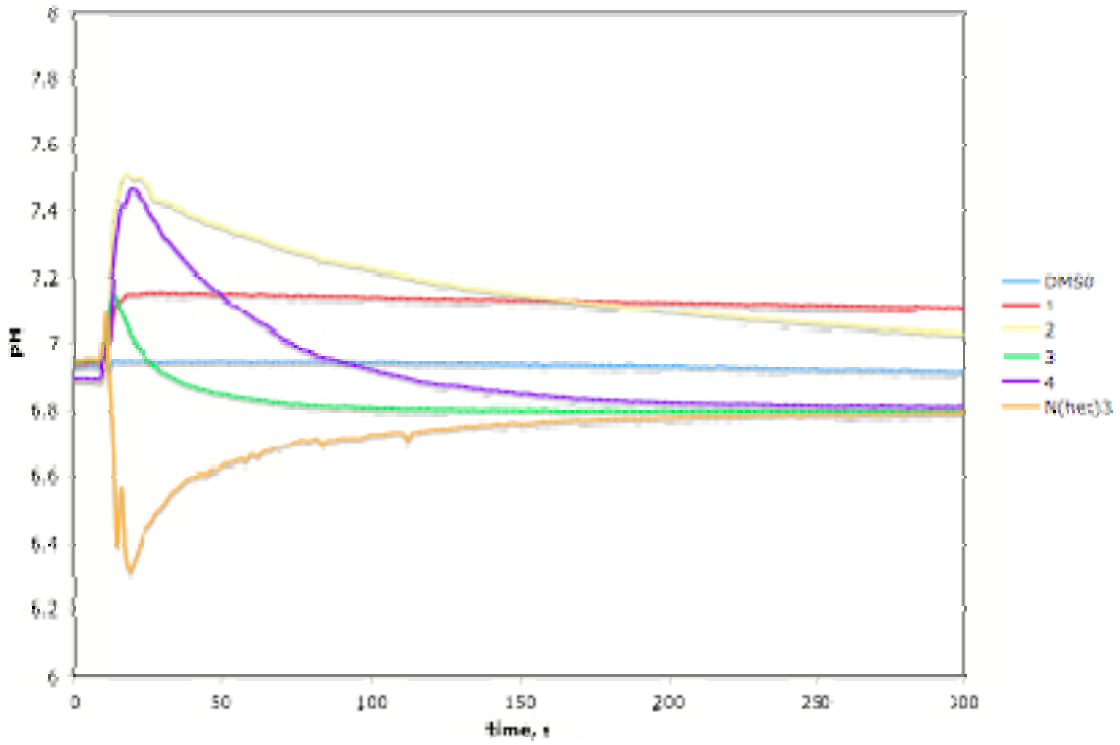

Figure S24 Change in intravesicular pH promoted by 0.04 molar equiv of receptors **1**-**4** and trihexylamine from unilamellar POPC vesicles loaded with 500 mM NaCl and 1 mM HPTS buffered to pH 6.9 with sodium phosphate salts. The vesicles were dispersed in 489 mM $NaNO_3$ buffered to pH 6.9 with 5 mM sodium phosphate salts. At the end of the experiment, detergent was added to lyse the vesicles. Each point represents the average of three trials

Discussion

Figure S22 indicates that addition of receptors **2**-**4** to a sample of vesicles containing 489 mM NaCl suspended in 167 mM Na_2SO_4 (all solutions buffered to pH 6.9 with sodium phosphate salts) results in an increase in internal pH. We attribute this response to the efflux of HCl mediated by these receptors, thus explaining the release of chloride observed in the corresponding ISE experiment. Compound **1** and trihexylamine were found not to mediate chloride efflux in this ISE experiment. Figure S23 shows that these compounds mediate only a small change in internal pH under these conditions. Thus it may be concluded that these compounds have much lower activity as HCl co-transporters.

We also investigated the internal pH change on addition of these receptors to a sample of vesicles containing 489 mM NaCl suspended in 489 mM $NaNO_3$ (all solutions buffered to pH 6.9 with sodium phosphate salts). The results are shown in Figure S24. We observed that compound **1** shows extremely similar behaviour to the previously described assay; that changing the external anion has no effect on the pH

change mediated by this receptor. Compounds **2**-**4** exhibit a different trend. Addition of these compounds initially causes the internal pH to increase; however, after a period of time the internal pH is observed to decrease and returns to close to the starting value. We attribute these results to an initial rapid period of HCl efflux; however, this leads to the establishment of a pH gradient causing the electrostatic potential inside the vesicle to rise which inhibits the HCl transport. After this point, observed chloride efflux is due to a chloride/ nitrate anti-port process which becomes the dominant mechanism. The pH gradient is reduced by the slower process of HNO_3 influx. This re-establishment of internal pH is only observed when nitrate is the external anion as it is not possible to transport sulfate (accompanied by protons) through the membrane due to Hofmeister bias.

Interestingly trihexylamine shows the opposite behaviour in this assay; that is the internal pH initially decreases followed by re-alkalinization. We propose that this is due to a preference for co-transport of HNO_3 over HCl by this receptor. Thus, initially HNO_3 is transported into the vesicle followed by the slower efflux of HCl. This preference would be expected on the basis of Hofmeister bias. Trihexylamine does not contain (thio)urea NH donors required to classically bind these anions so it is plausible that this results in a preference according to the Hofmeister series. However, when the external anion in sulfate (as in figure S23) this trend is reversed as efflux of HCl is the only available option.

Dependance of the HPTS response on pH

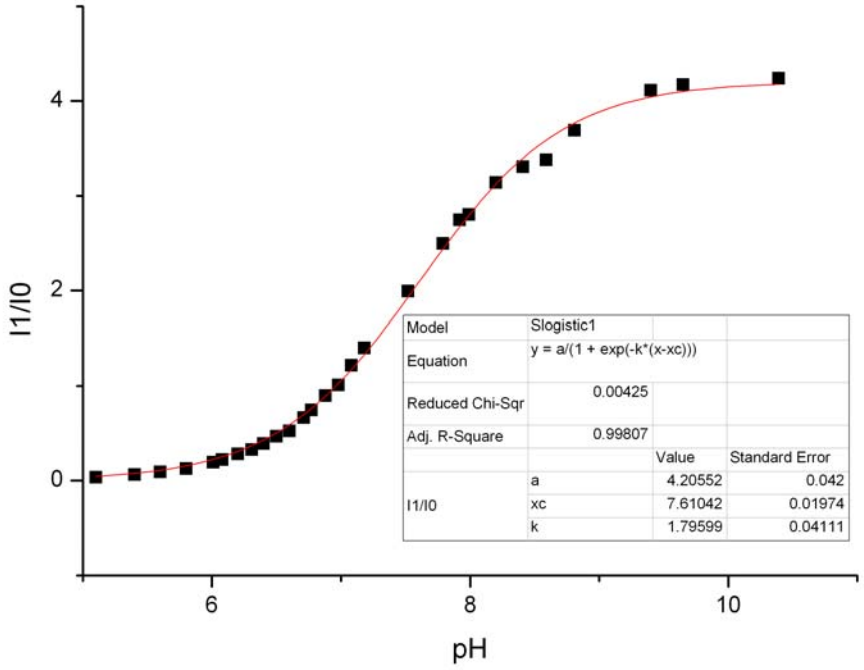

Figure S25 Dependence of I_1/I_0 on pH. I_1 and I_0 are the HPTS fluorescence emissions at 510 nm where I_1 is excitation at 460 nm (basic form of HPTS) and I_0 is excitation at 403 nm (acidic form of HPTS). This curve may be fitted to the following equation: pH= -1/1.796*(ln(4.2055/[I_1/I_0]-1))+7.6142

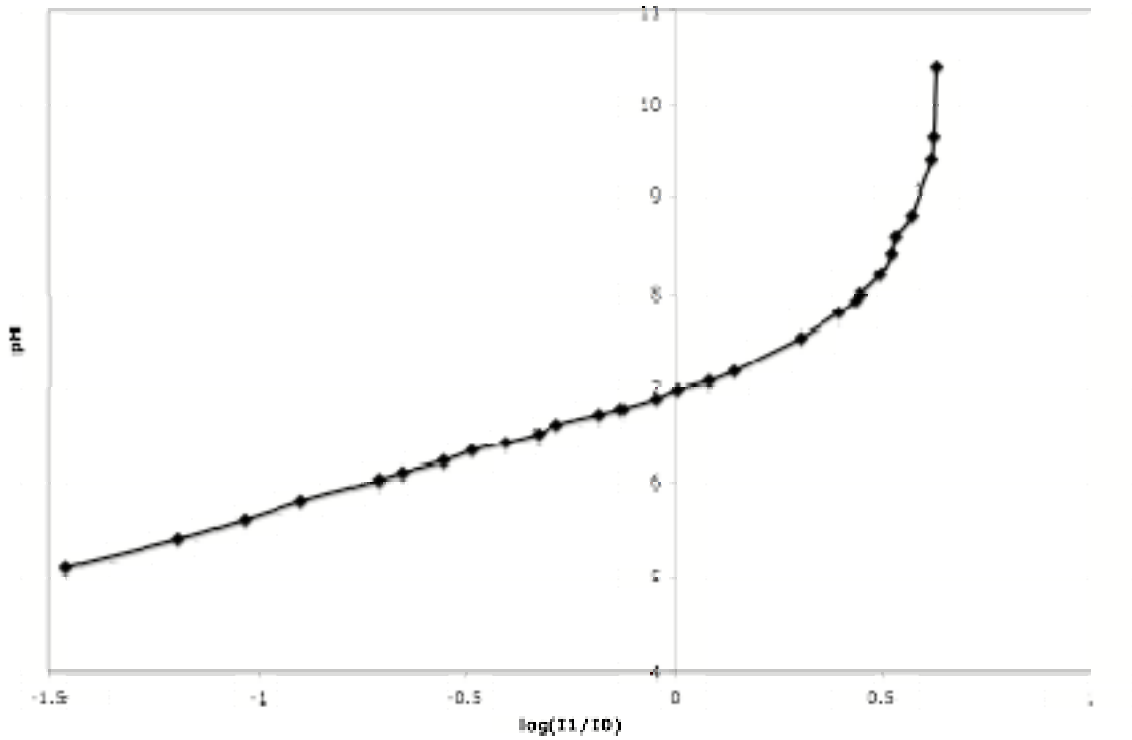

Figure S26 Dependence of $\log(I_1/I_0)$ on pH. I_1 and I_0 are the HPTS fluorescence emissions at 510 nm where I_1 is excitation at 460 nm (basic form of HPTS) and I_0 is excitation at 403 nm (acidic form of HPTS).

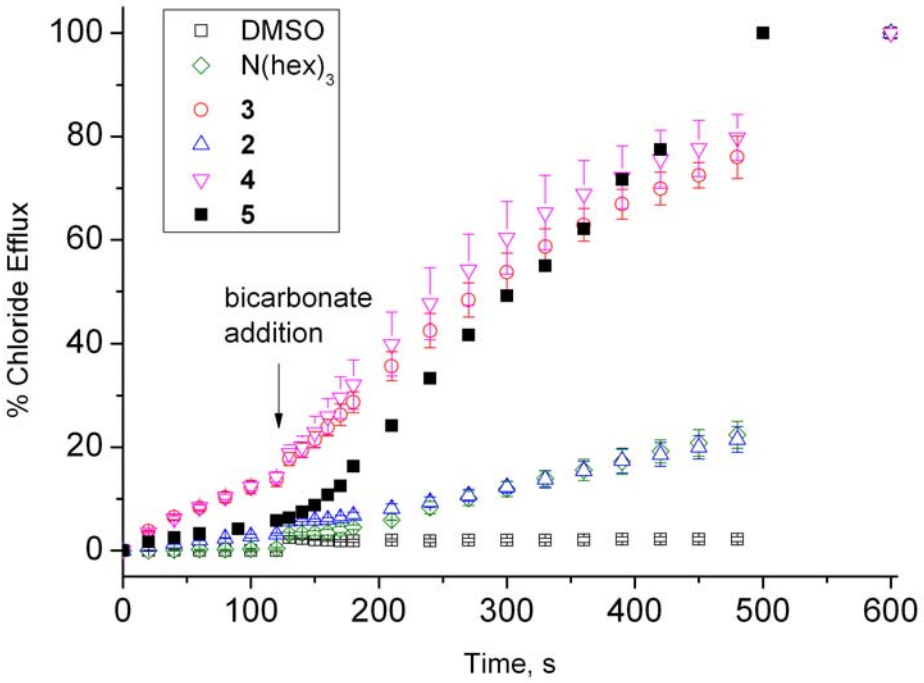

Figure S27 Chloride efflux promoted by 0.01 molar equiv of receptors **1**-**4**, isophtalamide **5**[11] and $N(hex)_3$ from unilamellar POPC vesicles loaded with 500 mM NaCl buffered to pH 7.2 with 20 mM sodium phosphate salts upon addition of a $NaHCO_3$ pulse to make the extravesicular bicarbonate concentration 40 mM. The vesicles were dispersed in 162 mM Na_2SO_4 buffered at pH 7.2 with 20 mM sodium phosphate salts. At the end of the experiment, detergent was added to lyse the vesicles and calibrate the ISE to 100% chloride release. Each point represents the average of 3 trials.

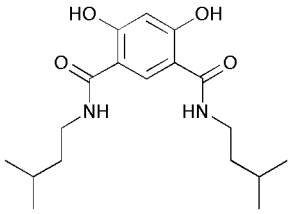

Figure S28 Isophtalamide **5** as published by Davis, Gale, Quesada and co-workers[11]

Comparison of release of chloride over time

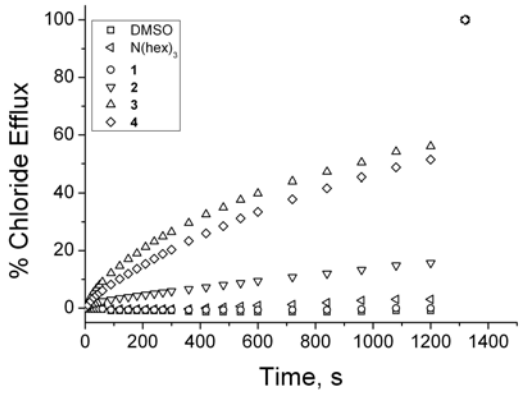

Figure S29 Chloride efflux promoted by 0.04 molar equiv of receptors **1**-**4** and N(hex)3 from unilamellar POPC vesicles loaded with 489 mM NaCl buffered to pH 7.2 with sodium phosphate salts. The vesicles were dispersed in 167 mM Na2SO4 buffered to pH 7.2 with 5 mM sodium phosphate salts. At the end of the experiment, detergent was added to lyse the vesicles and calibrate the ISE to 100% chloride release. Each point represents the average of three trials

Table S2 Stability constants (K_a/M^{-1})for compounds **1**-**4** with various TBA salts in DMSO-d_6/0.5% H_2O at 298K with error and resonance which was used to calculate stability constant. Average values are quoted if it was possible to follow more than one NH resonance. Errors < 15%.

Compound	TBA chloride	TBA nitrate	TBA sulfate	TEA bicarbonate
1	658	No significant interaction	$>10^4$ (NH at 5.88ppm)	Does not fit 1:1 binding model.
2	830	No significant interaction	$>10^4$	Does not fit 1:1 binding model.
3	447	No significant interaction	$>10^4$	564
4	191	No significant interaction	$>10^4$	Peak broadening

Figure S26 ^{1}H NMR titration in DMSO-d_6/H_2O 0.5% for compound **1** with various TBA salts. Changes in chemical shift are fitted to a 1:1 binding model.

a) Compound **1** with TBA chloride. NH at 5.88 ppm

K_a = 655 M^{-1} error =

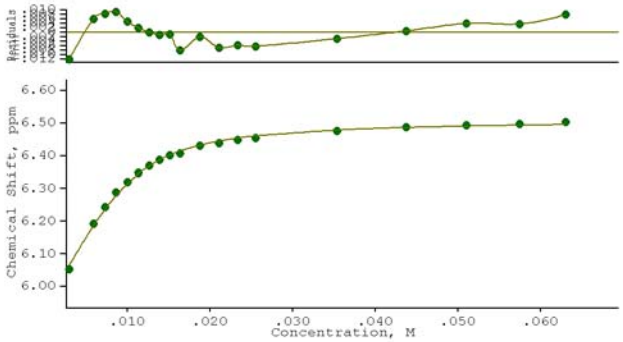

7%

b) Compound **1** with TBA chloride. NH at 5.80 ppm.

K_a = 661 M^{-1} error = 6%

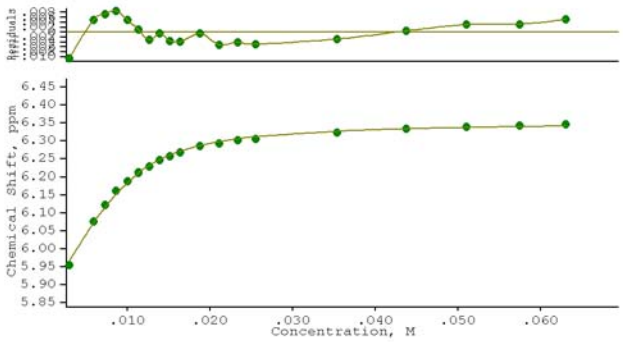

c) Compound **1** with TBA sulfate. NH at 5.88 ppm.

K_a >1x10^4 M^{-1}

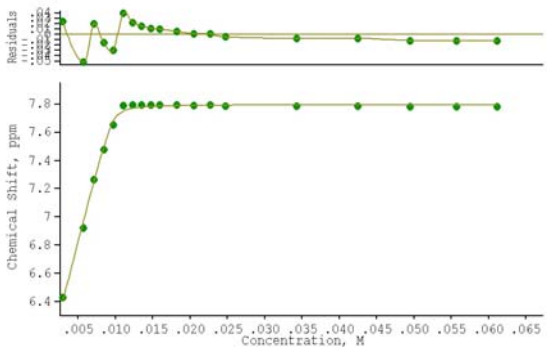

d) Compound **1** with TBA sulfate. NH at 5.80 ppm.

K_a >10^4 M^{-1}

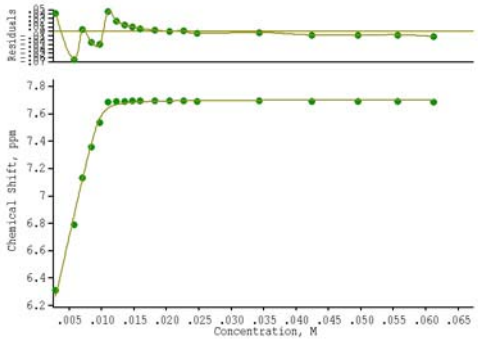

Figure S27 ^{1}H NMR titration in DMSO-d_6/H_2O 0.5% for compound **2** with various TBA salts. Changes in chemical shift are fitted to a 1:1 binding model.

a) Compound **2** with TBA chloride. NH at 8.50 ppm.

K_a = 777 M^{-1} error = 8%

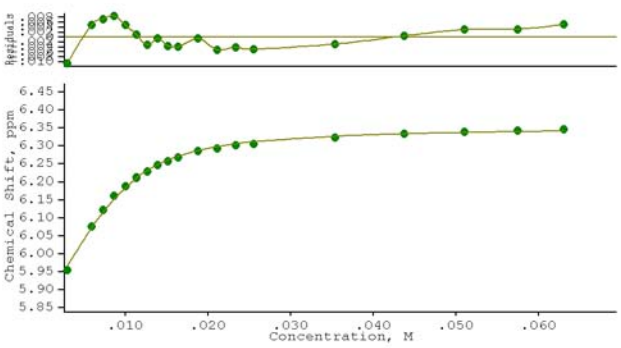

b) Compound **2** with TBA chloride. NH at 6.17 ppm.

K_a = 882 M^{-1} error = 7%

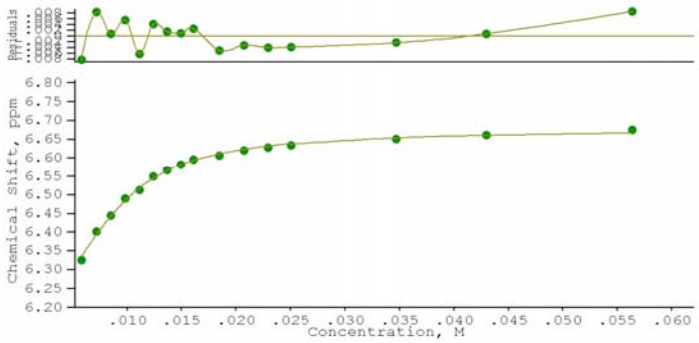

c) Compound **2** with TBA sulfate. NH at 8.50 ppm.

K_a >1x10^4 M^{-1}

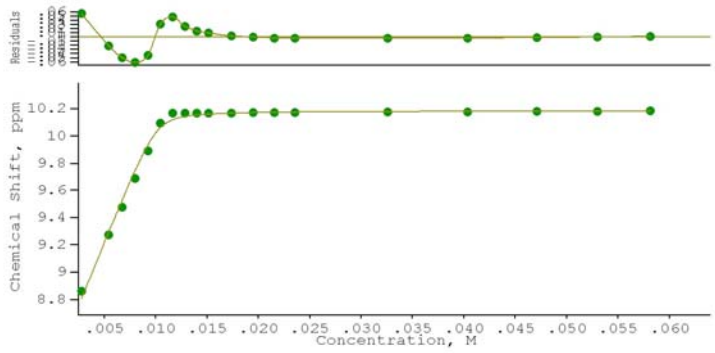

d) Compound **2** with TBA sulfate. NH at 6.17 ppm.

K_a >1x10^4 M^{-1}

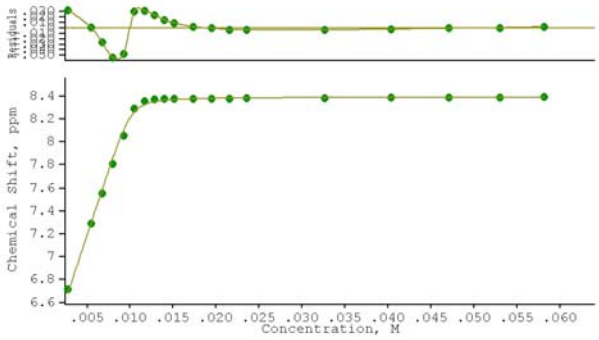

Figure S28 ^{1}H NMR titration in DMSO-d_6/H_2O 0.5% for compound **3** with various TBA salts. Changes in chemical shift are fitted to a 1:1 binding model.

a) Compound **3** with TBA chloride. NH at 7.48 ppm.

K_a = 440 M^{-1} error = 3%

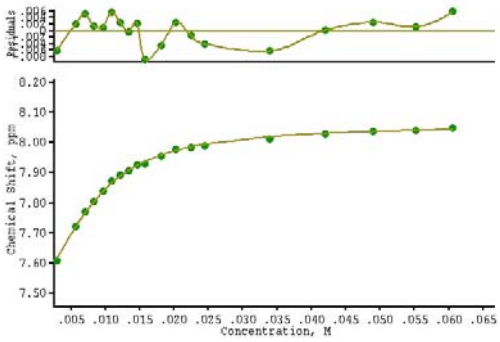

b) Compound **3** with TBA chloride. NH at 7.18 ppm.

K_a = 455 M^{-1} error = 4%

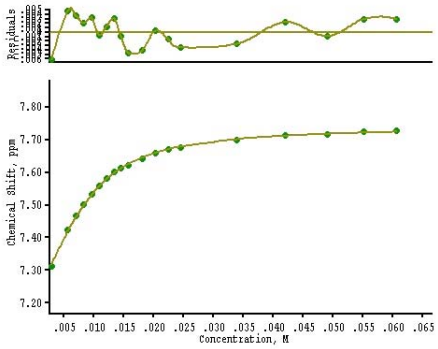

c) Compound **3** with TBA sulfate. NH at 7.48 ppm.

K_a >1x10^4 M^{-1}

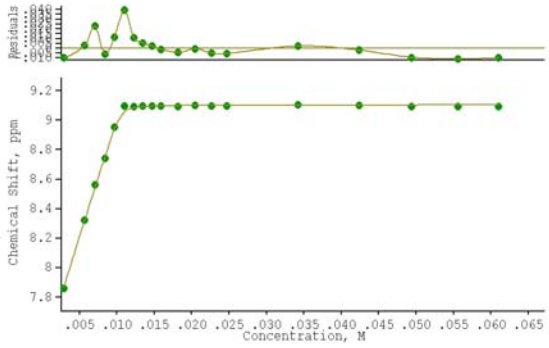

d) Compound **3** with TBA sulfate. NH at 7.18 ppm.

K_a >1x10^4 M^{-1}

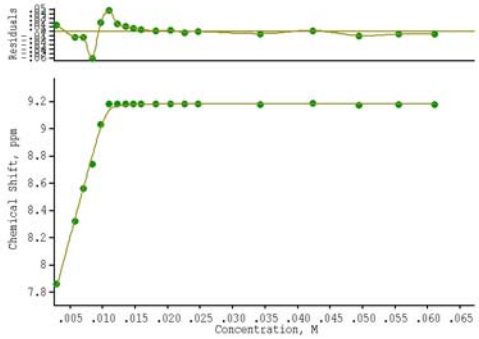

e) Compound **3** with TEA bicarbonate. NH at 7.47ppm.

K_a= 451 M^{-1} error = 8%

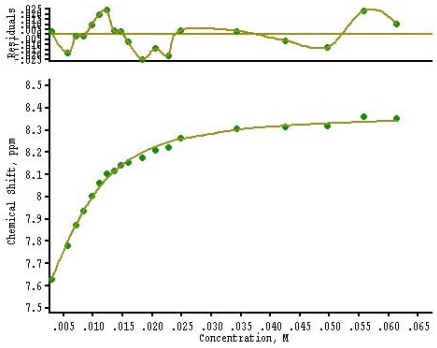

f) Compound **3** with TEA bicarbonate. NH at 7.18ppm.

K_a = 678 M^{-1} error = 9%

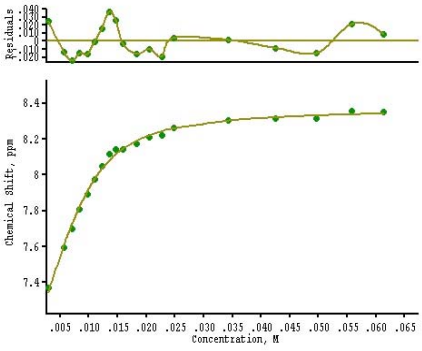

Figure S29 ^{1}H NMR titration in DMSO-d_6/H_2O 0.5% for compound **4** with various TBA salts. Changes in chemical shift are fitted to a 1:1 binding model.

a) Compound **4** with TBA chloride. NH at 9.59 ppm

K_a = 191 M^{-1} error = 13%

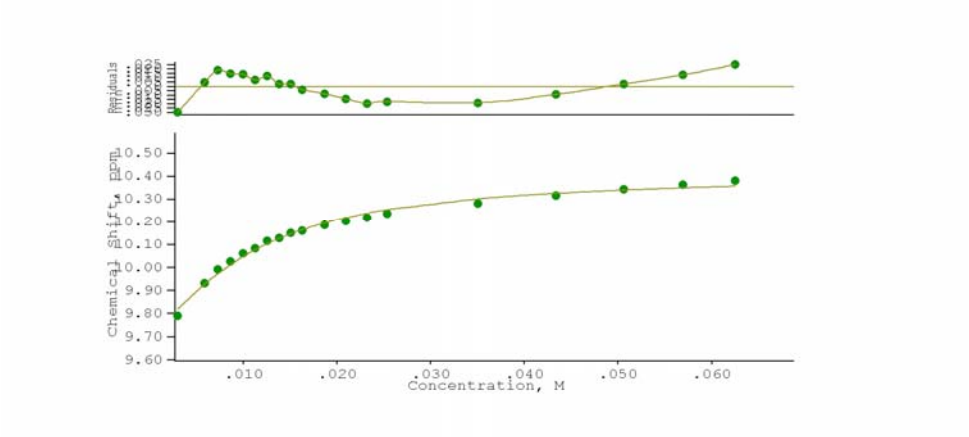

b) Compound **4** with TBA chloride. NH at 7.61 ppm.

K_a = 191 M^{-1} error = 13%

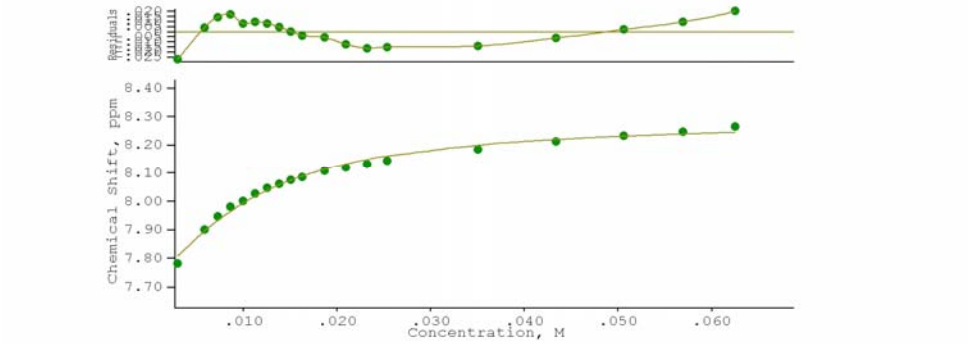

c) Compound **4** with TBA sulfate. NH at 9.60 ppm.

K_a >1x10^4 M^{-1}

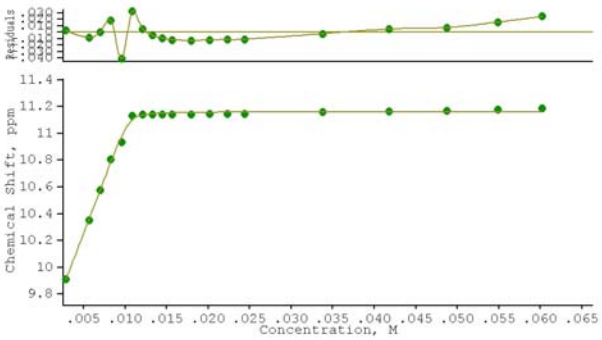

d) Compound **4** with TBA sulfate. NH at 7.60 ppm.

K_a >1x10^4 M^{-1}

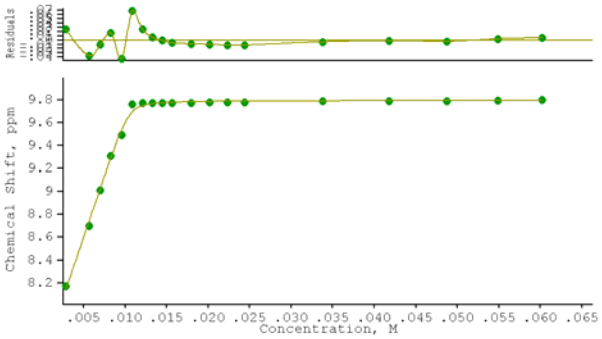

Figure S30 Job plots in DMSO-d_6 /0.5% H_2O for compound **1** with various tetraethylammonium bicarbonate

a) Compound **1** with TEA bicarbonate. NH at 5.78 ppm

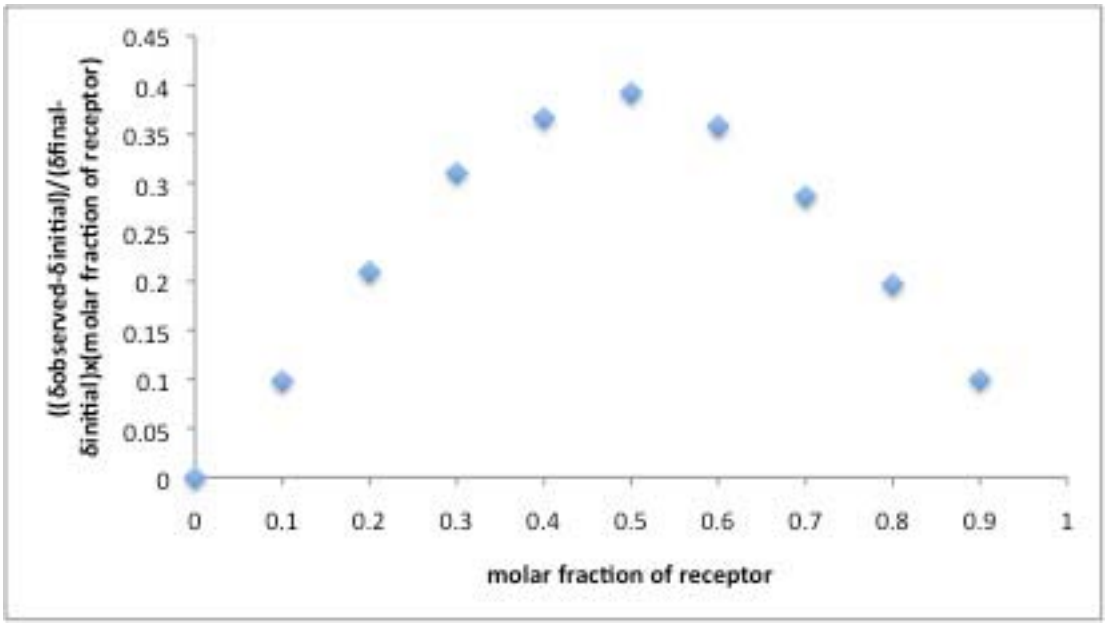

Figure S31 Job plots in DMSO-d_6 /0.5% H_2O for compound **2** with various tetraethylammonium bicarbonate

a) Compound **2** with TEA bicarbonate. NH at 8.50 ppm

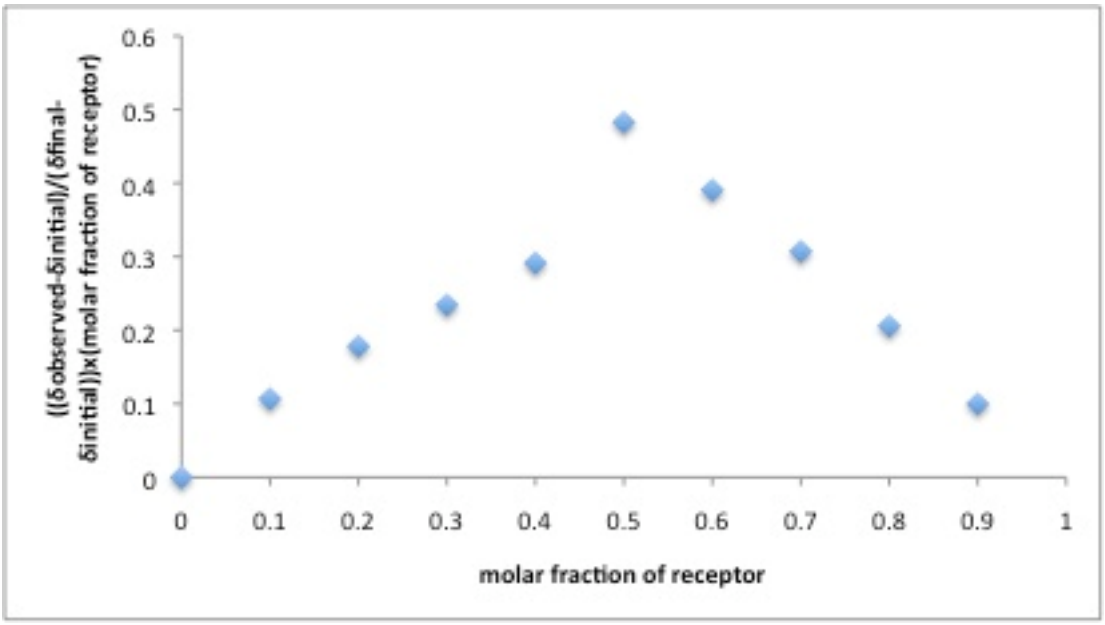

Figure S32 Job plots in DMSO-d_6 /0.5% H_2O for compound **3** with various tetrethylammonium bicarbonate

a) Compound **3** with TEA bicarbonate. NH at 7.47ppm

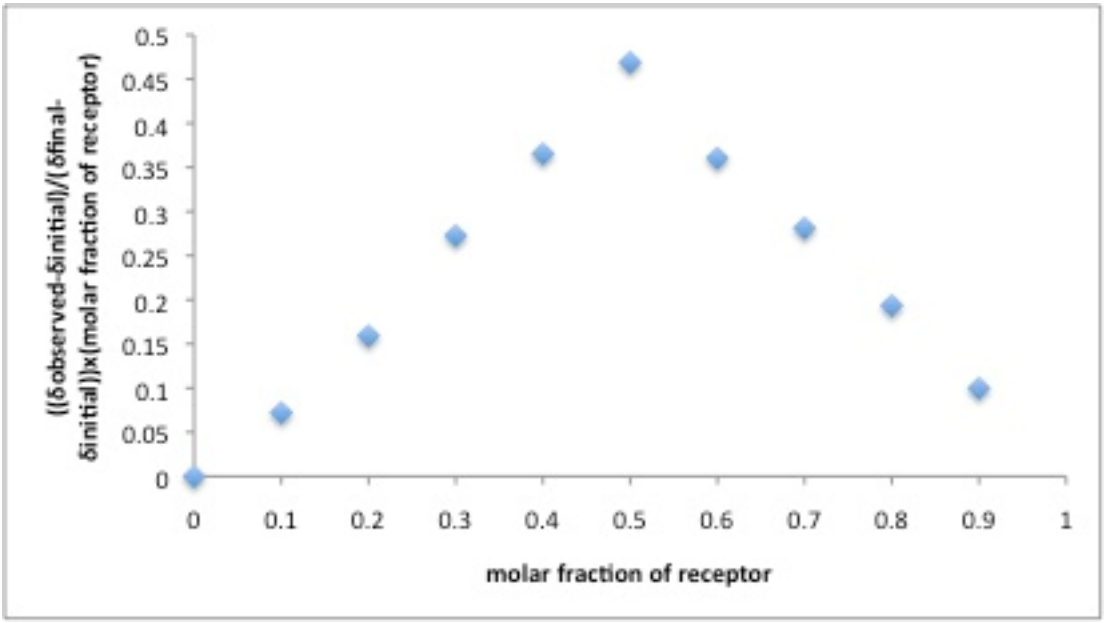

Figure S33 Stacked plots showing stepwise additions of (a) MeOH, (b) OH^- (c) HCO_3^- and OH^- and (d) HCO_3^- to compound **1** in DMSO-d_6 with 0.5% water.

(a)

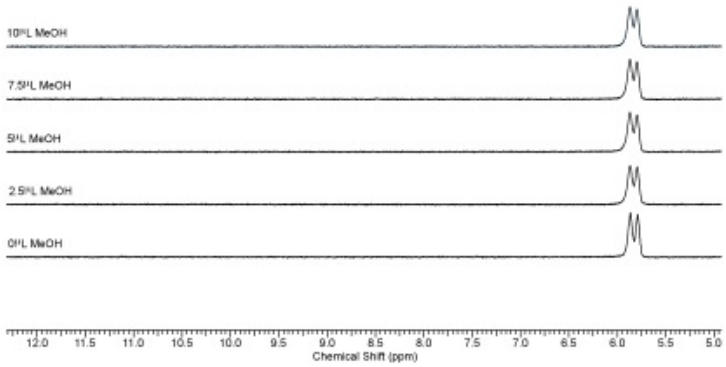

(b)

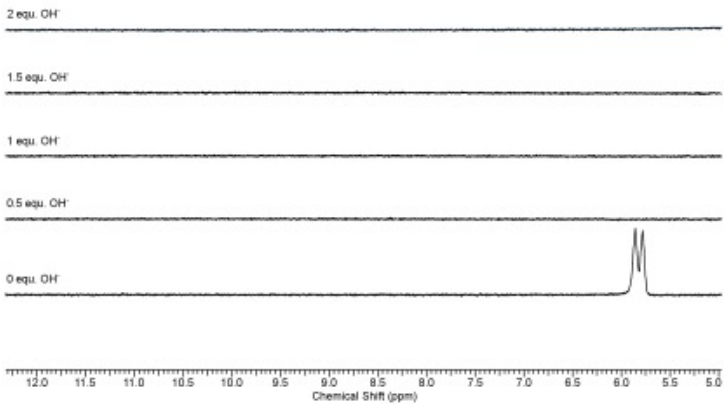

(c)

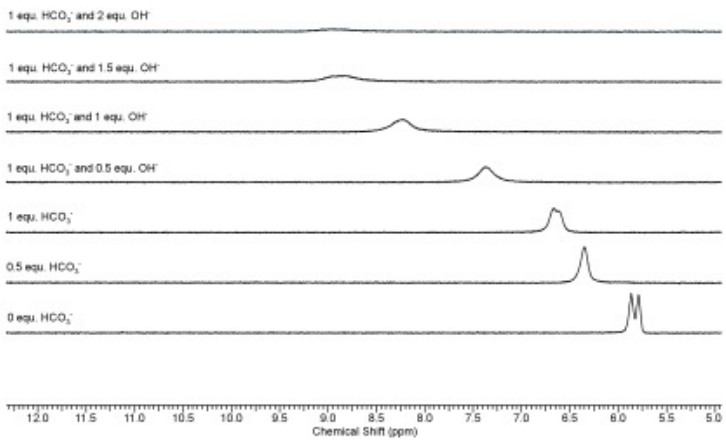
1 equ. HCO3- and 2 equ. OH-
1 equ. HCO3- and 1.5 equ. OH-
1 equ. HCO3- and 1 equ. OH-
1 equ. HCO3- and 0.5 equ. OH-
1 equ. HCO3-
0.5 equ. HCO3-
0 equ. HCO3-
12.0 11.5 11.0 10.5 10.0 9.5 9.0 8.5 8.0 7.5 7.0 6.5 6.0 5.5 5.0
Chemical Shift (ppm)

(d)

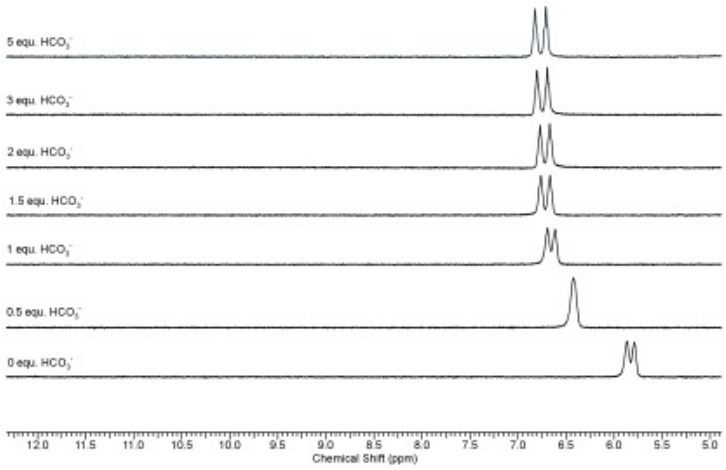
5 equ. HCO3-
3 equ. HCO3-
2 equ. HCO3-
1.5 equ. HCO3-
1 equ. HCO3-
0.5 equ. HCO3-
0 equ. HCO3-
12.0 11.5 11.0 10.5 10.0 9.5 9.0 8.5 8.0 7.5 7.0 6.5 6.0 5.5 5.0
Chemical Shift (ppm)

Figure S34 Stacked plots showing stepwise additions of (a) MeOH, (b) OH^- (c) HCO_3^- and OH^- and (d) HCO_3^- to compound **2** in DMSO-d_6 with 0.5% water.

(a)

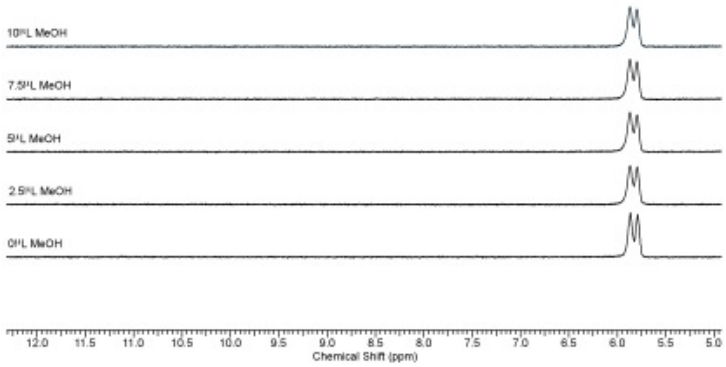

(b)

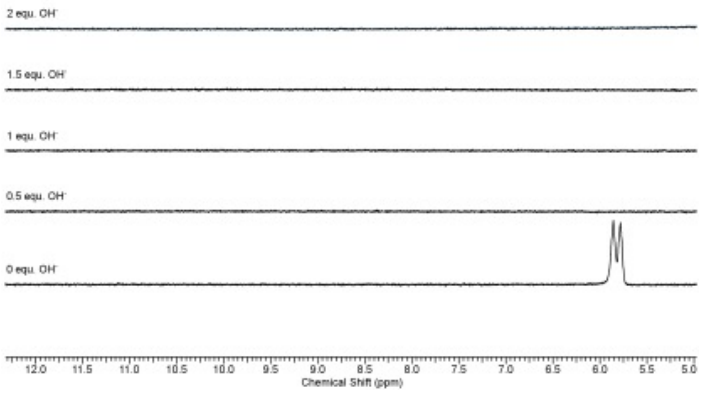

(c)

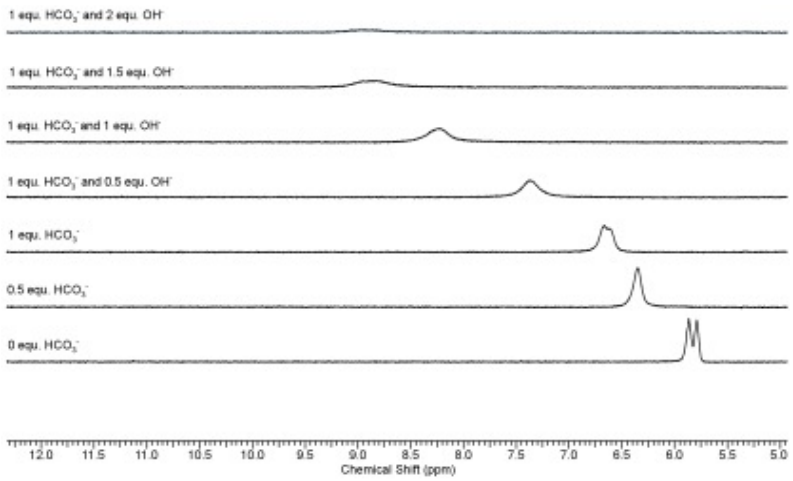
1 equ. HCO3- and 2 equ. OH-
1 equ. HCO3- and 1.5 equ. OH-
1 equ. HCO3- and 1 equ. OH-
1 equ. HCO3- and 0.5 equ. OH-
1 equ. HCO3-
0.5 equ. HCO3-
0 equ. HCO3-
12.0 11.5 11.0 10.5 10.0 9.5 9.0 8.5 8.0 7.5 7.0 6.5 6.0 5.5 5.0
Chemical Shift (ppm)

(d)

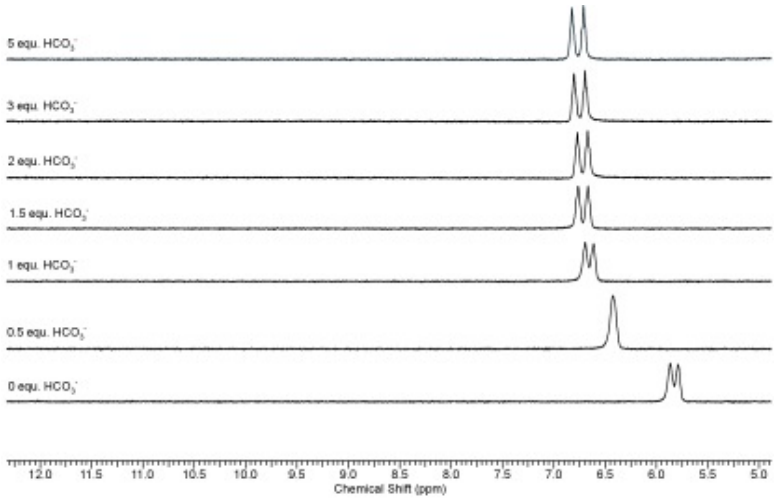
5 equ. HCO3-
3 equ. HCO3-
2 equ. HCO3-
1.5 equ. HCO3-
1 equ. HCO3-
0.5 equ. HCO3-
0 equ. HCO3-
12.0 11.5 11.0 10.5 10.0 9.5 9.0 8.5 8.0 7.5 7.0 6.5 6.0 5.5 5.0
Chemical Shift (ppm)

Figure S35 Stacked plots showing stepwise additions of (a) MeOH, (b) OH^- (c) HCO_3^- and OH^- and (d) HCO_3^- to compound **3** in DMSO-d_6 with 0.5% water.

(a)

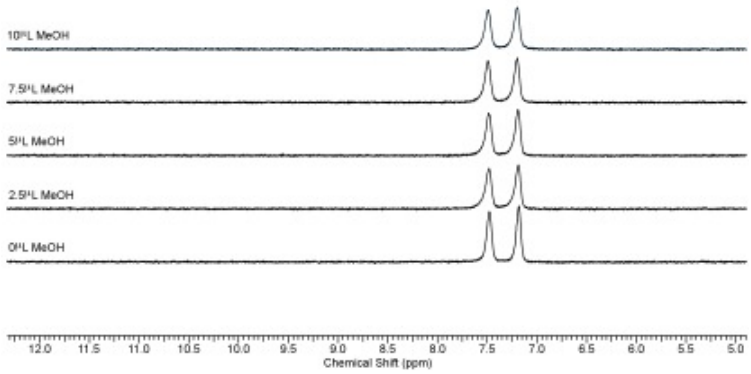

(b)

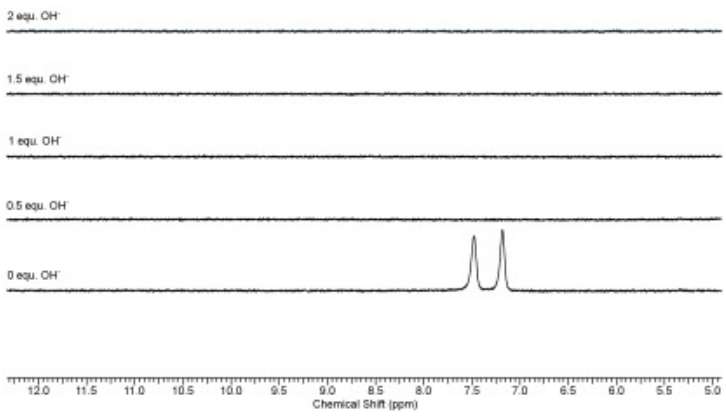

(c)

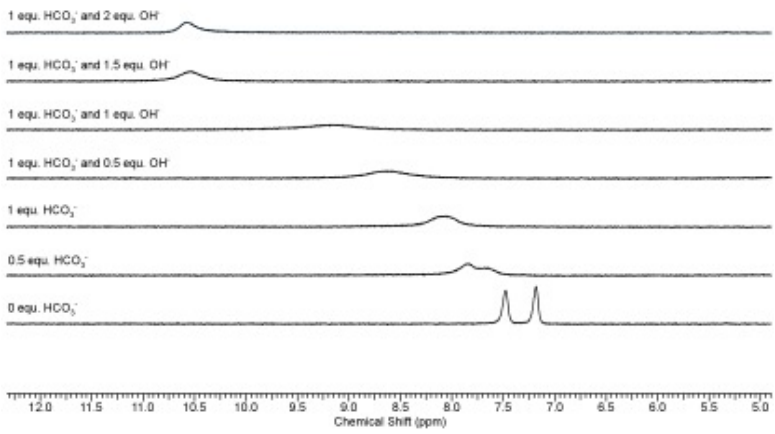
1 equ. HCO3- and 2 equ. OH-
1 equ. HCO3- and 1.5 equ. OH-
1 equ. HCO3- and 1 equ. OH-
1 equ. HCO3- and 0.5 equ. OH-
1 equ. HCO3-
0.5 equ. HCO3-
0 equ. HCO3-
12.0 11.5 11.0 10.5 10.0 9.5 9.0 8.5 8.0 7.5 7.0 6.5 6.0 5.5 5.0
Chemical Shift (ppm)

(d)

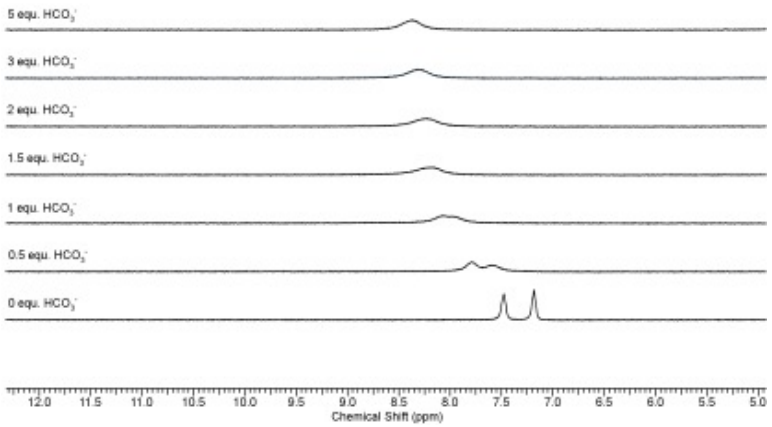
5 equ. HCO3-
3 equ. HCO3-
2 equ. HCO3-
1.5 equ. HCO3-
1 equ. HCO3-
0.5 equ. HCO3-
0 equ. HCO3-
12.0 11.5 11.0 10.5 10.0 9.5 9.0 8.5 8.0 7.5 7.0 6.5 6.0 5.5 5.0
Chemical Shift (ppm)

Figure S36 Stacked plots showing stepwise additions of (a) MeOH, (b) OH^- (c) HCO_3^- and OH^- and (d) HCO_3^- to compound **4** in DMSO-d_6 with 0.5% water.

(a)

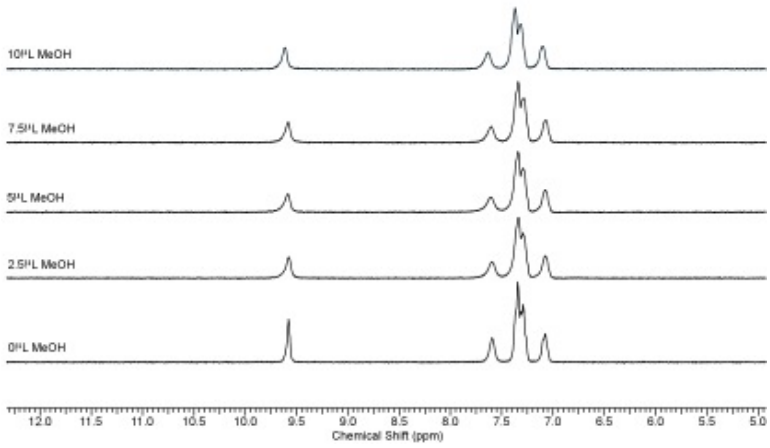

(b)

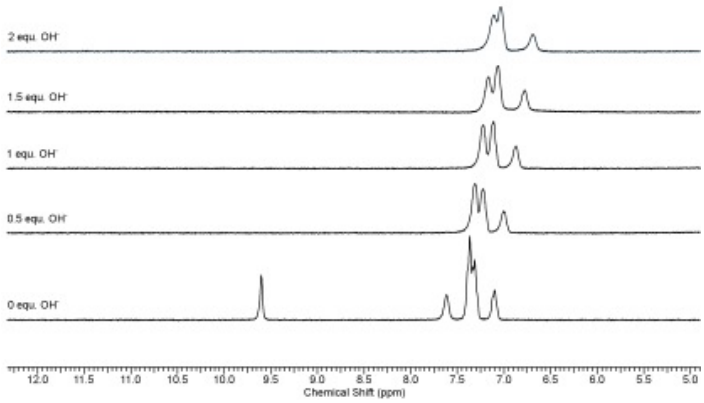

(c)

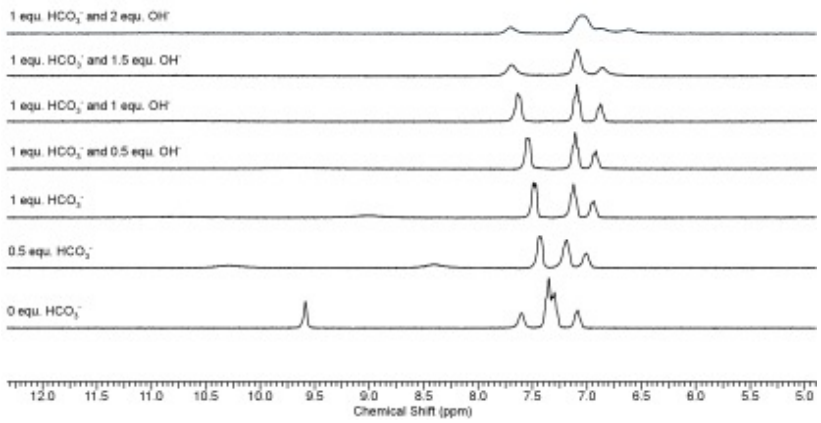
1 equ. HCO3- and 2 equ. OH-
1 equ. HCO3- and 1.5 equ. OH-
1 equ. HCO3- and 1 equ. OH-
1 equ. HCO3- and 0.5 equ. OH-
1 equ. HCO3-
0.5 equ. HCO3-
0 equ. HCO3-
12.0 11.5 11.0 10.5 10.0 9.5 9.0 8.5 8.0 7.5 7.0 6.5 6.0 5.5 5.0
Chemical Shift (ppm)

(d)

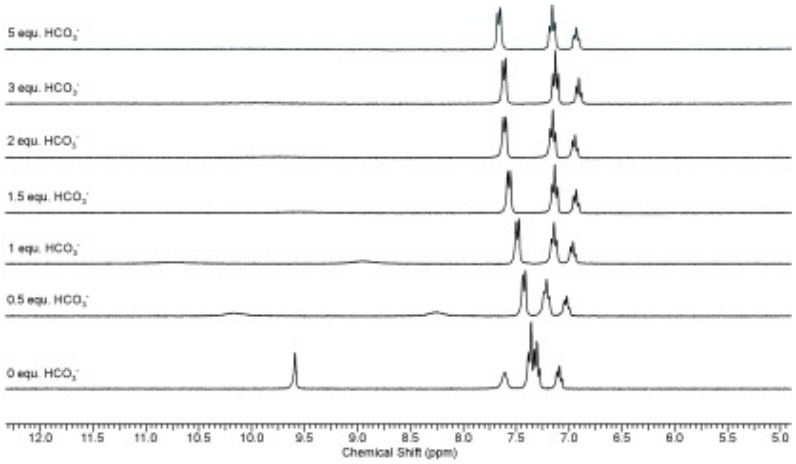
5 equ. HCO3-
3 equ. HCO3-
2 equ. HCO3-
1.5 equ. HCO3-
1 equ. HCO3-
0.5 equ. HCO3-
0 equ. HCO3-
12.0 11.5 11.0 10.5 10.0 9.5 9.0 8.5 8.0 7.5 7.0 6.5 6.0 5.5 5.0
Chemical Shift (ppm)

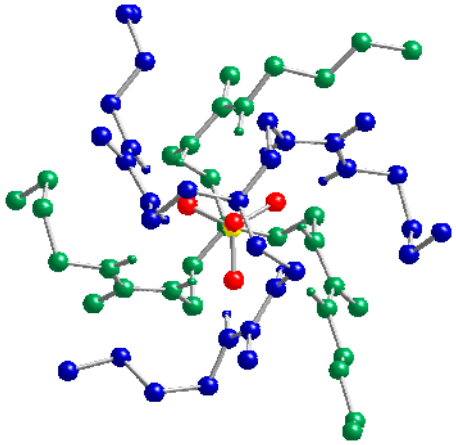

Figure S37 View of the sulfate complex present in the crystal structure of the tetrabutylammonium sulfate complex water solvate of receptor **1**.

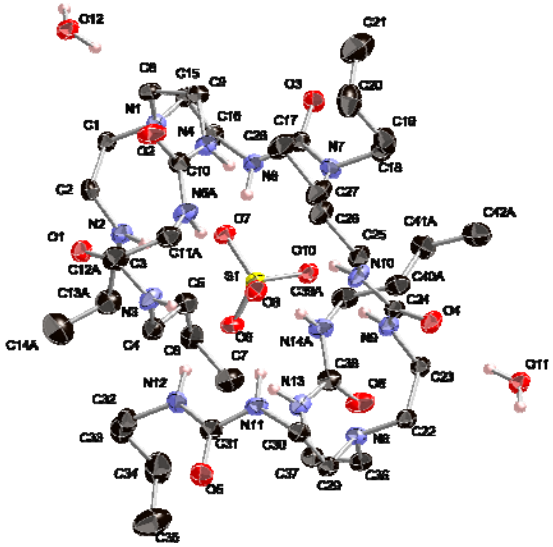

Figure S38 View of the sulfate complex present in the crystal structure of the tetrabutylammonium sulfate complex water solvate of receptor **1**. Thermal ellipsoids are drawn at the 35% probability level. Counter cations are omitted for clarity.

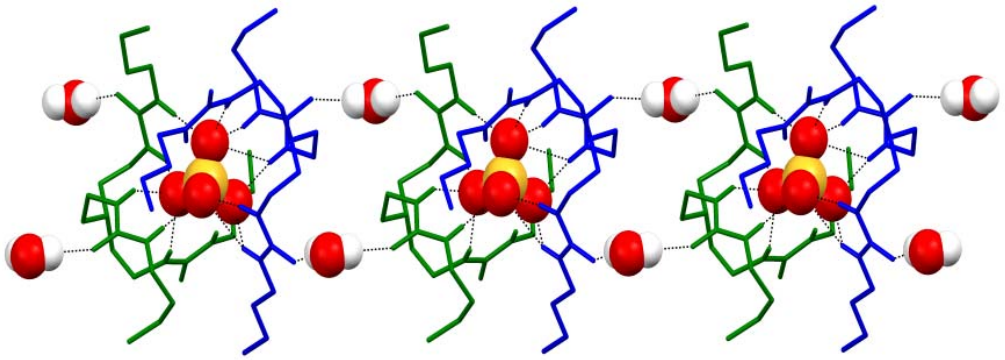

Figure S39 View showing water linked sulfate complexes in the solid state.

Crystallography – **1**.$TBA_2SO_4.2H_2O$

Crystal structure determination: Data were collected on a Bruker Nonius APEXII mounted at the window of an FR591 rotating Mo anode with confocal optics. Standard procedures were followed; thermal parameter and geometric restraints/constraints were applied to several disordered alkyl chains. Crystal data for **1**.$TBA_2SO_4.2H_2O$: M = 1504.29, Triclinic, a = 13.3171(4), b = 14.1510(6), c = 24.6875(10) Å, α = 90.1722(16)°, β = 103.847(3)°, γ = 90.899(2)°, U = 4516.5(3) $Å^3$, T = 120(2) K, space group $P\bar{1}$, Z = 2, μ = 0.097 mm^{-1}, 79090 reflections measured, 18486 unique reflections (R_{int} = 0.1410). The final R_1 values were 0.0757 ($I>2\sigma(I)$). The final $wR(F_2)$ values were 0.1687 ($I>2\sigma(I)$). The final R_1 values were 0.1687 (all data). The final $wR(F_2)$ values were 0.2075 (all data). The goodness of fit on F_2 was 1.006.

Table S3. Hydrogen bonds [Å and °] in the sulfate complex of receptor **1**.

D–H···*A*	*d*(*D*–H)	*d*(H···*A*)	*d*(*D*···*A*)	∠(*DHA*)
O12–H104···O1^{i}	0.855(17)	1.978(17)	2.814(3)	166(3)
O12–H103···O5^{ii}	0.834(17)	1.948(17)	2.772(3)	170(3)
O11–H102···O3^{iii}	0.840(17)	1.959(18)	2.779(3)	165(3)
O11–H101···O4	0.856(17)	1.952(19)	2.788(3)	165(4)
N2–H902···O7	0.88	2.14	2.872(3)	140.6
N3–H903···O9	0.88	2.06	2.932(3)	168.9
N4–H904···O7	0.88	2.21	2.891(3)	133.8
N6–H906···O7	0.88	2.24	2.955(3)	138.7
N7–H907···O10	0.88	2.06	2.924(3)	167.1
N5A–H5A1···O8	0.88	2.21	3.026(3)	154.7
N5A–H5A1···O7	0.88	2.49	3.229(3)	141.5
N9–H909···O10	0.88	2.02	2.898(3)	171.4
N11–H911···O8	0.88	2.16	3.013(3)	164.5
N12–H912···O9	0.88	2.15	2.914(3)	144.5
N13–H913···O9	0.88	2.22	3.044(3)	156.4
N10–H910···O8	0.88	2.25	2.962(3)	138.4
N14A–H14G···O10	0.88	2.23	2.952(4)	138.5
N14A–H14G···O9	0.88	2.52	3.291(4)	146.7
N14B–H14H···O10	0.88	2.44	2.952(4)	117.8
N14B–H14H···O9	0.88	2.53	3.291(4)	145.0

Symmetry transformations used to generate equivalent atoms:

(i) x+1,y+1,z (ii) x,y+1,z (iii) x+1,y,z

Crystallography $\mathbf{4}_2.(TEA)^2.CO_3^{2-}$ Data were collected on a Bruker Nonius

APEXII mounted at the window of an FR591 Mo rotating anode; standard data reduction and refinement procedures were used. Crystal data for $\mathbf{4}_2.(TEA)_2CO_3^{2-}$: M = 1424.08, Monoclinic, a = 24.1742(5), b = 24.4456(7), c = 12.7595(4) Å, β = 93.313(2)°, U = 7527.7(4) $Å^3$, T = 120(2) K, space group Cc, Z = 4, μ = 0.238 mm^{-1}, 33393 reflections measured, 15112 unique reflections (Rint = 0.0804). The final R1 values were 0.0856 (I>2σ(I)). The final wR(F2) values were 0.1532 (I>2σ(I)). The final R1 values were 0.1339 (all data). The final wR(F2) values were 0.1767 (all data). The goodness of fit on F^2 was 1.065. Flack parameter = 0.69(9) . The structure was refined as a racemic twin.

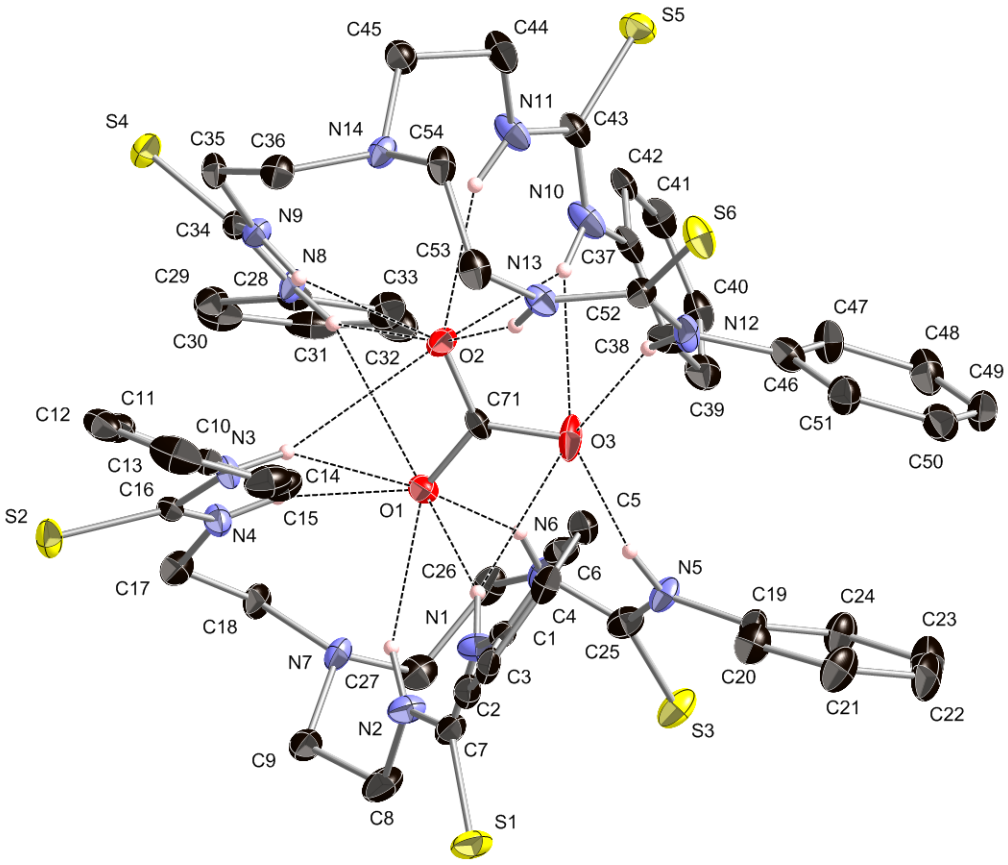

Figure S40 The X-ray crystal structure of the carbonate complex of receptor **4**. Thermal ellipsoids drawn at the 35% probability level. Counter cations are omitted for clarity.

Table S4. Hydrogen bonds [Å and °] in the carbonate complex of receptor **4**.

D–H···*A*	*d*(*D*–H)	*d*(H···*A*)	*d*(*D*···*A*)	∠(*DHA*)
N1–H901···O1	0.88	2.21	3.027(6)	155.1
N1–H901···O3	0.88	2.61	3.407(7)	150.6
N2–H902···O1	0.88	2.20	3.001(6)	152.0
N3–H903···O1	0.88	2.10	2.882(6)	147.2
N3–H903···O2	0.88	2.59	3.403(6)	155.0
N4–H904···O1	0.88	2.26	3.012(6)	142.8
N5–H905···O3	0.88	1.96	2.832(6)	169.8
N6–H906···O1	0.88	2.20	3.016(7)	153.5
N8–H908···O2	0.88	2.07	2.873(6)	151.3
N8–H908···O1	0.88	2.60	3.413(6)	153.1
N9–H909···O2	0.88	2.17	2.927(6)	143.7
N10–H910···O2	0.88	2.28	3.070(7)	150.0
N10–H910···O3	0.88	2.44	3.257(8)	154.3
N11–H911···O2	0.88	2.18	3.006(6)	155.7
N12–H912···O3	0.88	2.00	2.824(6)	155.4
N13–H913···O2	0.88	2.09	2.945(7)	163.2

References

1 R. J. Warr, K. J. Bell, A. Gadzhieva, A. J. Blake, M. Schroeder, A. N. Westra, J. Chartres, R. Ellis, C. Tong, T. G. Simmance and P. A. Tasker, *Chem. Eur. J.*, 2009, **15(19)**, 4836-4850

2 F. Werner and H-J. Schneider, *Helv. Chim. Act.*, 2000, **83(3),** 465-478

3 M. de Loos, G. J. Alette, J. v. Esch, H. Kooijman, A. L. Spek, R. Hage, R. M. Kellogg and B. L. Feringa, *Eur. J. Chem.*, 2000, **22**, 3675-3678

4 C. Raposo, M. Almaraz, M. Martin, V. Weinrich, L. M. Mussons *et al.*, *Chem Lett.*, 1995, **9**, 759-760

5 R. J. Warr, K. J. Bell, A. Gadzhieva, A. J. Blake, M. Schroeder, A. N. Westra, J. Chartres, R. Ellis, C. Tong, T. G. Simmance and P. A. Tasker, *Angew. Chem. Int. Ed.*, 2008, **47(9)**, 1745-1748

6 M. Wenzel, K. Gloe, G. Bernhard, J. K. Clegg, X-L Ji and L. F Lindoy, *New. J. Chem.*, 2008, **32(1)**, 132-137

7 K-Y Jeong, K-M Hahn and Y. L. Cho, *Tett. Lett.*, 1998, **39 (22)**, 3779-3782

8 HPTS assay as reported by S. K. Berezin and J. T. Davis, *J. Am. Chem. Soc.*, **2009**, *131*, 2458-2459

9 Reviews: (a) T. M. Fyles, *Chem. Soc. Rev.*, 2007, **36**, 335. (b) N Sakai, J. Mareda and S. Matile, *Mol. BioSystems*, 2007, **3**, 658.

10 (a) P. H. Schlesinger, R. Ferdani, J. Liu, J. Pajewska, R. Pajewska, M. Saito, H. Shabany and G. W. Gokel, *J. Am. Chem. Soc.*, 2002, **124**, 1848. (b) A. V. Koulov, T. N. Lambert, R. Shukla, M. Jain, J. M. Bood, B. D. Smith, H. Y. Li, D. N. Sheppard, J. –B. Joos, J. P. Clare and A. P. Davis, *Angew. Chem. Int. Ed.*, 2003, **42**, 4931. (c) J. L. Sessler, L. R. Eller, W.–S. Cho, S. Nicolaou, A. Aguilar, J. T. Lee, V. M. Lynch and D. J. Magda, *Angew. Chem. Int. Ed.*, **2005**, *44*, 2989. (d) P. V. Santacroce, J. T. Davis, M. E. Light, P. A. Gale, J. C. Iglesias-Sanchez, P. Prados and R. Quesada, *J. Am. Chem. Soc.*, 2007, **129**, 1886

11 J. T. Davis, P. A. Gale, O. A. Okunola, P. Prados, J. C. Iglesias-Sanchez, T. Torroba and R. Quesada, *Nat. Chem.*, 2009, **1**, 138